UNIVERSITY OF BIRMINGHAM

University of Birmingham

Cold and ultracold molecules in the twenties

Softley, Timothy P.

Link to publication on Research at Birmingham portal

Author for correspondence:
Timothy P. Softley
e-mail: t.p.softley@bham.ac.uk

Cold and ultracold molecules in the twenties

Timothy P. Softley

School of Chemistry, University of Birmingham, Edgbaston, Birmingham B15 2TT, UK

TPS, 0000-0002-5285-6308

A diversity of experimental techniques has been developed over the last 25 years to create samples of molecular gases at temperatures close to the Absolute Zero—here we consider samples in the range from 10s of Kelvin (cold) down to 10s of nanoKelvin (ultracold). In these exotic physical environments, a range of novel experiments can be conducted which bring high levels of control over the properties of these 'almost stationary' molecules, in some cases with control over single trapped molecules achievable. In this article, recent advances in this field since 2020, both in terms of the ability to produce and manipulate the molecules and understand their properties, and also in the development of new applications of these technologies, are highlighted. Applications include observing explicit 'quantum effects' in chemical reactivity, developing an understanding of chemistry in cold astrophysical media, the creation of exotic phases of matter, the use of trapped molecules in quantum computation and simulations systems, and the use of very high-precision spectroscopic measurements to answer fundamental physics questions beyond the standard model of particle physics.

1. Introduction

This article discusses some recent developments in the study of cold and ultracold molecular gases: we consider how they are created and interrogated; what we understand about their properties; and how those properties may be controlled to enable a range of scientific and technological applications. Such applications include studying quantum effects in chemistry; modelling astrophysical chemistry; making precision measurements for fundamental physics by high-resolution spectroscopy; using trapped molecules

as qubits or 'qudits' for quantum information and simulation; and studying condensed matter intermolecular interactions and physics on a measurable length and timescale, of relevance to novel materials and exotic phases of matter. In this article, we refer to molecular gases as 'cold' in the temperature range from 10s of Kelvin down to 1 mK, or 'ultracold' at sub-mK temperatures down to 10s of nanoKelvin—this definition reflects more the different experimental techniques that are used in each range rather than an abrupt boundary in the properties of the gases in these two ranges. In both ranges, the gases are maintained at low density in order to avoid condensation to a solid or liquid, and the molecules are trapped or confined within an ultra-high vacuum (UHV) apparatus, so that they are isolated from collisions with thermal (room temperature) gas molecules and with the walls of the apparatus.

The distinguishing features of cold and ultracold molecular gases, which make them so interesting to study, may include the following (depending to some extent on the temperature and the molecular system):

(i) The molecules are moving very slowly—they have low velocity, low momentum and low kinetic energy—and hence the amount of time they spend in a given spatial region is long, allowing longer interrogation times and more sensitive detection methods. Spectroscopic line broadening due to the optical Doppler effect and 'transit-time line broadening' is much reduced. It may even be possible to trap, interrogate and manipulate single molecules within the cold gas.

(ii) The *relative* velocity of different molecules within a given sample is low—hence collisions between those molecules are less frequent and less energetic. At the lowest ultracold temperatures, we will need to use a fully quantum wave-motion description of such collisions and interactions, rather than considering particles bumping into one another (see below). In addition, the orbital angular momentum associated with colliding pairs of molecules—proportional to the relative velocity—is low, and the quantization of that angular momentum has important consequences for the physics of low-temperature collisions.

(iii) The population of internal quantum states—the vibrational, rotational, fine-structure (e.g. electron spin-rotation or spin-orbit coupling), hyperfine-structure (nuclear spin and nuclear multipole moment) states—is confined to a few states, or even just one state of the molecules. This will allow an exquisite degree of control over properties such as the orientation of the electric or magnetic dipole moment of the molecules, and also allows entanglement of quantum states within molecules or between pairs of molecules. If the molecules are tightly confined by a trap, then the motional quantum states within the trap will also need to be considered and controlled.

(iv) Low temperature also implies a lower entropy, and hence it may be possible to organize the molecules into regular 'structures' or arrays (e.g. using an optical standing-wave field, or in a Coulomb crystal of ions [1]), and there may also be the opportunity to create coherent multi-molecule quantum states of the system e.g. in a Bose–Einstein condensate. This enables the study and application of highly controlled interactions between the molecules, as well as exotic properties.

Cold molecular gases are an important component of the astrophysical medium, and many different molecules have been detected in the extremely low-density environment (10^0–10^4 molecules cm^{-3}) of interstellar gas clouds at temperatures of order 10–50 K [2]. However, *ultracold* molecular gases (less than 1 mK) do not exist as such in nature, and indeed there are no known environments in the Universe where the temperature has been measured as below 1 K—the lowest-temperature object observed is the Boomerang Nebula with an average temperature around 1 K [3], while the cosmic microwave background is measured at around 2.7 K. Thus, our understanding of cold and, particularly, ultracold molecular gases is largely derived from laboratory measurements and theory. Following the remarkable progress from the 1970s onwards in producing ultracold samples of *atoms*, principally alkali metals, at temperatures as low as the

nanoKelvin regime—using techniques such as laser cooling, evaporative cooling, optical and electromagnetic trapping [4]—physicists and chemists set out to develop methods capable of producing cold *molecular* samples and this has been a very active and creative field since the 1990s. The first 20 or so years of development of the field were reviewed by Bell & Softley [5], and even by then, many new cold-molecule production methods had been developed. By contrast to laser cooling of atoms, where around 30 elements (mainly metallic, some with isotopic variants) have been laser cooled [6] and another 10 or so non-metallic elements (e.g. H, O, N, Br) cooled by other methods, the number of molecular species that could be considered for cooling is almost unlimited, at least in principle. As the cold-molecule field was developed, it was anticipated that the diverse chemistry of molecular species, the existence of molecular electric dipole and higher multipole moments (anisotropic charge distributions), the potential for creating cold chiral species, and the complex energy structure of molecules (derived from the vibration and rotational degrees of freedom) would be a rich feeding ground for novel physics and chemistry.

Broadly speaking, two categories of methods have been developed to produce cold and ultracold molecules—'Direct' and 'Indirect'. In the Direct approaches, one starts with a sample of the molecules of interest and then uses one or more of a number of methods to reduce the temperature (or the mean energy—see below) of the sample—these include using electromagnetic fields to slow down the molecules, laser (Doppler) cooling, immersion in cryogenically cooled gases (e.g. He or Ne), or velocity selection of the low-velocity tail of the velocity distribution of a thermal sample. For the Indirect approaches, one produces ultracold samples of atoms (normally) and then uses association techniques, using laser-driven transitions or ramped magnetic fields, to convert those samples into ultracold molecules through the chemical bonding of the atoms; further cooling is likely to be applied to convert the molecules into the lowest quantum state (see §2 and table 1 for further details and references).

The concept of 'temperature'—and consequently what we mean by 'cooling'—requires careful consideration. In a classical gas, the temperature is a measure of the spread of energies in the various molecular degrees of freedom, which for translational motion follows a Maxwell–Boltzmann distribution of kinetic energies. 'Cooling' implies reducing the spread of energies while maintaining thermal equilibrium. In general, such equilibrium requires sufficient collisions on the relevant experimental timescale, but this is not the case for many of the experiments discussed here. For example, in experiments working with low-density 'collision-free' molecular beams, the cold gas samples are not produced in conventional thermal equilibrium. Nevertheless 'temperature' (or 'effective temperature') is frequently used in the literature as a proxy for the mean energy of the molecules $T \sim \langle E \rangle / k_B$ (where k_B is the Boltzmann constant), or equivalently the literature refers to a mean energy expressed in units of Kelvin. In that sense, non-equilibrium molecular gases may be described as having a different 'temperature' in different motional degrees of freedom, and therefore we may choose to define a T_{rot}, T_{vib} or T_{trans} representing the mean energy in the rotational, vibrational and translational degrees of freedom, respectively. Lowering the temperature also generally implies a decrease in entropy, and that underlies the challenge in 'working against thermodynamics' to produce these samples at sufficient densities to do useful experiments. An important concept in the field, related to the entropy, is that of the phase-space density—given by the number of particles per cubic de Broglie wavelength [58], with the de Broglie wavelength λ given by the de Broglie equation of particle-wave duality $p = h/\lambda$ (see below). As the mean momentum of the molecules p decreases with temperature, the wavelength increases, and if the number density of molecules stays constant then the phase-space density will increase. Strictly speaking, we do not 'cool' a sample unless the phase-space density is increased; hence for example, simply separating out the slowest molecules from a thermal sample does not generally increase phase-space density. True cooling, therefore, requires a mechanism to dissipate energy without decreasing the density—and hence a reduction in the entropy.

A key aspect of these cold and ultracold molecular samples, hinted above, is the transition to a fully quantum regime as the sample is cooled. At room temperature, we already describe the electrons in molecules in terms of wave functions (spatially dispersed orbitals) but typically describe the translational motion of the overall molecule in classical terms. The de Broglie

Table 1. Summary of methods for producing cooling and trapping cold and ultracold molecules.

technique	principle	applicability (molecules, temperature, quantum states)	references
direct methods			
laser cooling of molecules	Using detuned laser light, transitions are driven in a closed optical cycle, resulting in molecule-to-photon momentum transfer, with spontaneous emission producing energy dissipation leading to net cooling.	Requires accessibility of strong spectroscopic transitions in IR, visible or near-UV ranges. A closed optical cycle for molecules occurs only when there is little geometry change between ground and excited states (diagonal Franck–Condon factors for vibrational change), e.g. CaF, TiO, YO, CaOH. Temperatures down to microKelvin range. Normally, single internal quantum-state cooled.	[7] and references in §2a
evaporative cooling	Pre-cooled molecules are held in a trap and then the trap depth is lowered in a sequence of steps, with time for thermal equilibration between each step. Hotter (more energetic) molecules leave the trap, cooling the sample.	Requires dominance of elastic collisions over inelastic collisions in the sample—demonstrated, e.g. KRb, OH. MilliKelvin to nanoKelvin range and applicable to single quantum state (which is initially trapped).	[8,9]
Stark and Zeeman deceleration	Molecules in a beam pass through a sequence of inhomogeneous pulsed fields (Stark $=$ electric field, Zeeman $=$ magnetic field) and are progressively slowed down in each pulse by the potential energy hill that is created. Alternatively, molecules in the beam are trapped in a moving electric or magnetic trap (created in a sequence of static electrodes or coils), and then the velocity of the trap is reduced.	Stark - requires strong dipole moment and ideally linear Stark effect, e.g. ND_3, OH, CH, CH_3F, NO. Zeeman - strong magnetic moment (paramagnetic species - hence normally unpaired spin/radical species) e.g. O_2, CH_3. MilliKelvin range achievable. Single quantum state decelerated, and normally low-field seeking states only (energy increases with field). Stark deceleration has also been applied to molecules in Rydberg states.	[10,11] [12,13] [14,15]

(*Continued*.)

Table 1. (*Continued.*)

5

technique	principle	applicability (molecules, temperature, quantum states)	references
electrostatic velocity selection	Dipolar molecules are passed continuously as a beam (sometimes from a cryogenic buffer gas cell—see below) into a quadrupole or hexapole guide with one or more bends. As the molecules reach the bend only the slow-moving molecules pass the bend while faster molecules overshoot the bend and are lost. Thus only the low-velocity tail of the initial thermal distribution is transmitted through the guide.	Applied to dipolar molecules with a significant Stark effect, e.g. NH_3, CH_3F, H_2O. A related technique can be used to separate molecular conformers with different dipole moments. Only molecules in low-field seeking states are guided. The internal temperature (T_{rot}, T_{vib}) of the output beam may be similar to the input beam—hence use of cryogenic beams. Some spatial alignment of the output beams has been demonstrated.	[16–19]
	Magnetic velocity filter guides have also been demonstrated using permanent magnets.		[20]
cryogenic buffer gas cooling	Molecules are injected into (or created within) a cryogenically cooled gas (typically He at 400 mK to a few Kelvin in temperature) and thermally equilibrate with the cold gas by collisions. In some cases (see above), the molecules are ejected from the buffer gas cell as a cryogenic beam into an electrostatic or magnetic guide, or subsequent cooling device.	Wide range of species including molecules produced by laser desorption (e.g. SrF). However, trapping or guiding of cooled molecules requires magnetic/electric moment. Early experiments trapped paramagnetic molecules in a magnetic trap within the buffer gas-cooled region. Temperatures as low as 400 mK achieved—determined by cryogenic gas temperature. Thermal distribution across internal energy states at or near cryogenic gas temperature.	[21]
inelastic collisional cooling	Inelastic collisions between species at crossing point of two molecular beams lead to almost stationary species left behind at the crossing point.	Applicable to limited number of cases where the inelastic energy transfer in the collision balances (cancels) the lab-frame beam velocity e.g. NO, NH_3.	[22]

(*Continued.*)

Table 1. (*Continued*.)

6

royalsocietypublishing.org/journal/rspa   *Proc. R. Soc. A* **479**: 20220806

technique	principle	applicability (molecules, temperature, quantum states)	references
mechanical cooling—rotating wheel	A molecular beam valve is mounted on a rotating wheel, such that the backward tangential velocity of the valve is equal and opposite to the forward supersonic beam velocity.	In principle applicable to any molecule that can be created in a simple supersonic beam, provided the beam velocity can be matched by the rotating wheel velocity (potentially difficult for very light molecules such as H_2, or for radicals created by photolysis or discharge)	[23,24]
	A 'centrifuge decelerator' was reported in 2014 in which molecules are guided electrostatically towards the centre of a rotating wheel and are slowed by centrifugal forces as they move to the centre of the wheel.	Applied to molecules with dipole moment e.g. CH_3F.	[25]
sympathetic cooling with laser-cooled gases	A trap of pre-cooled molecules is merged with trapped laser-cooled atomic gases, and collisions lead to cooling and equilibration of the molecules at the lower temperature.	Has only been demonstrated in a very few examples, e.g. LiNa cooled by Li, where there is a high ratio of elastic to inelastic collision cross sections. Temperatures as low as 220 nK achieved.	[26]
	For positive ions, even molecular ions that are not pre-cooled can be sympathetically cooled by laser-cooled Coulomb crystals.	Internal degrees of freedom are not generally cooled in the Coulomb crystal environment	[1,27]
Sisyphus cooling	Pre-cooled molecules (*ca* 400 mK) move within a novel inhomogeneous electric field trap, such that they slow down as they reach the edge of the trap and are then driven by microwaves to a level with a weaker Stark shift—and hence do not recoup the original kinetic energy on returning to the trap centre.	Applied to polyatomic molecules with a dipole moment. Demonstrated for CH_3F.	[28]

(*Continued*.)

Table 1. (*Continued*.)

technique	principle	applicability (molecules, temperature, quantum states)	references
indirect methods			
photoassociation	Pairs of laser-cooled atoms are photoexcited at the point of collision such that they form a bound excited-state dimer molecule—this is subsequently cooled to ground state by fluorescence or stimulated emission pumping (e.g. stimulated Raman adiabatic passage—STIRAP)	Applied to the association of alkali atoms to make diatomic species at ultracold temperatures (sub-mK). Molecules initially created in highly excited vibrational and electronic states, but can be cooled to ground state by coherent Raman pumping, hence single quantum state produced. MicroKelvin temperature range. Technique largely superseded by Magnetoassociation, which has higher efficiency.	[29,30]
magnetoassociation (Feshbach resonance)	Laser-cooled atoms are exposed to a ramped magnetic field such that those pairs of atoms on the point of collision are driven into a molecular-bound state as the field is ramped. Generally followed by optical Raman pumping to produce ground-state molecules.	Molecules ultimately in rovibrational ground state after STIRAP pumping. Principally applied to form dimers of alkali metals or alkaline earth atoms. Implementation requires detailed information on the Feshbach resonance behaviour of specific molecules.	[31–34]
		Temperatures in the microKelvin range achievable, and is currently the method of choice for ultracold experiments with alkali dimers.	
		Progress has been made towards magnetoassociation of ion–atom pairs.	[35]
photodissociation (Photostop)	Molecules are produced by photodissociation of parent molecules in a molecular beam, such that the photofragment recoil velocity cancels the parent velocity to produce very slow fragments in the laboratory frame of reference.	Has been applied to trap SH radicals and Br atoms. Requires favourable threshold photodissociation scheme (equalizing the excess velocity on photolysis, with the beam velocity)	[36,37]

(*Continued*.)

Table 1. (*Continued*.)

technique	principle	applicability (molecules, temperature, quantum states)	references
cooling in a moving frame			
merged beam	Two molecular beams with almost identical velocity are merged into a single beam (using a magnetic or electric sector to bend the path of one beam into the path of the other) so that the relative velocity of collisions between the species in the original beams is very low.	Merging generally requires the use of a curved electrostatic or magnetic sector to deflect one beam into the path of the other—hence a magnetic dipole or electric dipole is required for one molecular species. Principally applied to ionizing collisions (Penning ionization of He or Ne metastable atoms with a range of small species (e.g. H_2). Collision energies as low as a few milliKelvin achieved with high energy resolution.	[38]
Rydberg + neutral merged beams	One species excited to a high Rydberg state (e.g. principal quantum number $n = 30$) in a supersonic beam is guided into path of a neutral ground-state molecular beam. Collisions occur within the merged beam at low relative energy.	Effective translational temperatures down to *ca* 70 mK achieved; rotational temperatures are as achieved in a supersonic beam—3–10 K. The reaction of the Rydberg species with neutrals is effectively behaving as the corresponding ion–molecule reaction with the Rydberg electron as a spectator. Applied to reactions of $H_2(n)$ ($\equiv H_2^+$) and He(n) ($\equiv He^+$) with e.g. NH_3, HD, CH_3F.	[39] and references in §3a(i)
	Related approach applied to study energy transfer between a Rydberg atom and the rotational energies of a molecule has also been demonstrated.	Applied to e.g. NH_3 + He(n)	[40]
single molecular beam	Supersonic beams generally have low temperature in the moving frame of reference. Multiple species can be created in the beam to produce samples with low relative velocity and hence low-energy collisions.	Temperatures (relative energy) of a few Kelvin achievable. Likely to work well only with molecules of a similar mass, to avoid beam slippage and velocity spread.	[41,42]

(*Continued*.)

Table 1. (*Continued.*)

9

technique	principle	applicability (molecules, temperature, quantum states)	references
trapping techniques			
magneto-optical trap (MOT)	The MOT (the workhorse of atomic laser cooling experiments) applies a combination of counter-propagating circularly polarized cooling lasers in three orthogonal directions, with magnetic field coils. The Zeeman effect creates an imbalance in the strength of the laser-cooling (photon scattering) force within the trap with the net effect of pushing molecules (or cooled atoms) back to the centre.	Can only be used for molecular species that are laser cooled. YO, CaF, SrF have been trapped in MOTs, and recently the first example of a polyatomic species CaOH. Dual-species MOTs are also being developed currently (e.g. for CaF and Rb).	[43–45] [46]
electrostatic trap	In experiments with e.g. a Stark decelerator, an electrostatic trap can be used to confine the output of the dipolar molecular beam. An electromagnetic gate is required to admit molecules to the trap and then close the gate.	Typically trapping of polar molecules at temperatures in the milliKelvin range are achieved. Multiple loading (from multiple gas pulses) is challenging. Can be combined with an overlapped MOT or magnetic trap.	[47,48]
optical dipole trap	'far-detuned' laser beam attracts molecules (through the dipole force—ac Stark shift) into the laser focus.	Optical traps are generally relatively shallow compared to other types (*ca* 10 mK deep)—hence only ultracold species are likely to be trapped in this way, e.g. CaF, KRb, etc.	[49]
optical tweezer	Optical tweezers have tight radial confinement from a single-focused laser and are capable of trapping single molecules and translating their positions using opto-acoustic deflectors.	The trapping volume is of order 1 µm. Molecules can either be transferred from another trap into the tweezer (e.g. KRb) or pairs of ultracold atoms brought together in merged tweezers (e.g. LiCs).	[50]
optical array	The interference between two or more laser beams (or a single beam and its retro-reflection) can be used to create a standing wave which is an optical array of potential energy minima in 2 or 3 dimensions allowing trapping of an array of molecules.	Typical spacing of molecules in the array is 0.5—10 µm, and again only applicable to ultracold species.	

(*Continued.*)

Table 1. (*Continued*.)

technique	principle	applicability (molecules, temperature, quantum states)	references
magnetic trap	A set of coils arranged to produce a field minimum in three dimensions is used to confine molecules with a magnetic moment (low-field seeking state only). Alternatively, permanent or superconducting magnets create a field with a deep energy minimum for paramagnetic molecules. These have also been used to guide paramagnetic species (radial confinement).	In atomic laser cooling experiments, magnetic traps may be used in conjunction with evaporative cooling to push temperature down into the nanoKelvin regime. Can be operated across cold and ultracold temperature regimes, depending on magnetic field strength.	[43,51–54]
ion trap—Paul and other multipole traps	Paul trap (quadrupole) consists of four parallel rod electrodes to which a radiofrequency trapping field is applied, with electrostatic end caps for trapping in the axial direction. May be combined with laser cooling of atomic ions in the trap.	Widely applicable to trapping of both negative and positive molecular ions. Very deep traps possible—eV energy range. Laser cooling of trapped ions has only been applied to atomic species (e.g. Be^+, Ca^+, Mg^+ Yb^+) but sympathetic cooling of molecular ions can occur (see above). Temperature is generally limited by micromotion of ions in the radiofrequency field to mK lower limit.	[1]
	22-pole trap has benefit of much flatter central region of potential hence lower trap micromotion and has been used in conjunction with cryogenic buffer gas cooling.	22-pole trap with cryogenic cooling allows reaction or spectroscopic studies of wide range of molecular ions (Including large biomolecular species) down to a few Kelvins—including negative ions.	[55–57]

wavelength of a N_2 molecule (mass $m = 28$ u), moving at the RMS speed of $v = 520\,\mathrm{m\,s^{-1}}$ in a room temperature gas, is approximately 0.03 nm (using $mv = h/\lambda$) and is generally much smaller than the range of chemical bonding forces (0.1–0.3 nm) and very much smaller than the average separation of molecules in the gas. Hence much of gas kinetics and chemical dynamics can be described, qualitatively at least, in terms of classical collisions of particles (i.e. the molecules). As the temperature is lowered, the de Broglie wavelength varies in proportion to $T^{-1/2}$, such that at 'cold' temperatures of e.g. 30 mK the wavelength for N_2 is around 3 nm and at ultracold temperatures e.g. 3 μK is 300 nm, and we, therefore, expect the wave aspects of the wave-particle duality equation to come to the fore—the quantum regime. Ultimately, when the wavelength becomes comparable with inter-molecular separation—corresponding to a phase-space density of unity—the regime of 'quantum degeneracy' should be reached, with phenomena such as Bose–Einstein condensation (BEC) [59] occurring. Achieving quantum degeneracy of a molecular gas has been a major target of ultracold molecular science since the inception of the field—and as yet has only been achieved for fermionic (half-integral spin) molecular gases, not for bosonic (integral spin) gases.

In this article on 'Cold and ultracold molecules in the twenties', I will review the state of play of this field in the 2020s, highlighting some recent developments published from 2020 to early 2023. While the emphasis of this review is on *experimental* developments, this is an area where experiment and theory work hand in hand to understand the properties of matter in a 'quantum regime'. This review does not seek to give a fully comprehensive coverage of everything that has been achieved in this field, (see for example [1,7,11,15,58,60–70] for other recent relevant reviews, post-2015), but rather some case studies of new experiments have been selected because they point to future directions for this field. For the most part, we will be talking about 'small molecules' made of just a few atoms—diatomics, and small polyatomics—although prospects for studying more chemically complex species will be discussed.

It should also be remembered that 'the 20s' of other centuries have provided important developments, without which the research in the 2020s would not have been possible. In particular, the development of quantum mechanics in the 1920s (words such as 'quantum mechanics' and 'photon' were coined in the 1920s) lays a foundation for much of what has been achieved in the cold and ultracold molecule field since: the de Broglie hypothesis, the Heisenberg uncertainty principle, the first quantum chemistry theory of H_2 (Heitler and London), the Dirac equation and the development of quantum field theory, were among key discoveries of the 1920s. The phenomenon of BEC was already predicted by Einstein in 1924–1925. Key experimental developments, such as the Stern–Gerlach experiment in 1922 [71], have been exploited in the modern cold-molecule field by using inhomogeneous magnetic fields to control atomic and molecular motion for paramagnetic particles [69,70], and in the development of molecular beam methodologies using inhomogeneous electric fields [11,15]. The observation of electron diffraction in the Davisson–Germer experiments in 1923–1927 not only confirmed the de Broglie relationship but was also an early example of imaging electrons to reveal an interference pattern using a movable detector.

A century earlier, the 1820s was a time when some of the basic principles of electromagnetism were being developed—Orsted's observation of the magnetic field generated by a current-carrying wire; the 'right-hand rule' (Ampere); the research of Henry into the magnetic fields generated by coils. Hamilton's principle of varying action was applied in optics. It was also an important time for low-temperature science with the work of Carnot (the Carnot cycle) hinting towards the second law of thermodynamics, the liquefaction of chlorine by Faraday led to the mechanical method of refrigeration, and Coriolis coined the term 'kinetic energy' in the 1820s. In the 1720s, Fahrenheit proposed his scale of temperature having just invented the mercury thermometer, while in the 1620s the earliest known examples of the compound microscope first appeared in Europe. Thus, the world of cold and ultracold molecules builds very much on the legacy of the '20s' of the last four centuries, predating even the Royal Society of London!

In §2 of this article, I highlight some key recent experimental developments including advances in laser cooling of molecules, evaporative cooling of dipolar gases, and the use of optical tweezers

and arrays for trapping and manipulating molecules. In §3, applications in the areas outlined at the start of this section will be discussed, while §4 offers a brief outlook for the remainder of the decade.

2. The development of experimental techniques for studying cold and ultracold molecular gases

The key elements of any cold or ultracold molecule experiment may need to include methods for:

— Cooling or slowing the molecules (Direct), or producing the low-temperature molecules (Indirect)—including cooling their internal quantum state distribution (e.g. the vibration–rotation states, and the fine and hyperfine spin states).
— Optimizing the density of the sample—for almost any study, the ability to detect, manipulate and study interactions between molecules will be enhanced by controlling the density, and high phase-space density is a requirement for quantum-degenerate behaviour.
— Trapping or confining the slow-moving molecules spatially—generally using a combination of optical, electric and/or magnetic fields—so that they may be held and observed for a period long enough to interrogate their behaviour. Sometimes this involves confinement within a moving frame of reference, such as a molecular beam. In selected cases, it involves confining molecules into a regular one-, two- or three-dimensional lattice created by an optical standing wave, or into a tightly confined optical tweezer trap, with single molecules occupying a well-defined set of potential energy minima.
— Manipulating the quantum states of the molecules—often aimed at producing molecules uniquely in the ground quantum state (the lowest electronic–vibrational–rotational–hyperfine quantum level) and producing superposition states and entanglement. In a chemical context, there is also interest in being able to arbitrarily select a variety of specific internal quantum states to study the chemical behaviour as a function of quantum state.
— Detecting the molecules and characterizing the sample—its density, temperature, evolution with time; observing the (sometimes) localized positions of the particles; quantum-state detection.
— Detecting products of collisional scattering processes or other 'loss' processes (i.e. loss from the trapping zone)—e.g. reactive or inelastic collisions or radiative decay—including the directional properties of the post-collision trajectories of the product species.
— Determining coherence times and lifetimes of the prepared states, trapping times and reaction times (rates).
— Controlling the interactions between the molecules, for example by controlling the magnitudes or relative orientations of the molecular dipole moments.

The principles of slowing, cooling and trapping molecules have been well reviewed (see e.g. [5,65]). Table 1 summarizes some of the most frequently deployed methods and their range of applicability currently. None of the methods listed in table 1 are truly 'universal methods' that are capable of controlling temperature (or energy) across the full cold and ultracold ranges for any molecule. Indeed, because such processes use molecule-specific properties—such as dipole moments, polarizabilities, magnetic moments, masses, optical transition frequencies and radiative lifetimes—many cold/ultracold molecule experiments in laboratories around the world are designed for one specific molecule or a narrow range of molecules. Most of the techniques are also applicable only in fairly narrow temperature/energy ranges, and have variable success in cooling the different internal degrees of freedom of molecules. As indicated in table 1, in some cases the internal state distribution of the cooled species is 'thermal', but in most cases, the molecules may be partly or fully quantum state selected, or there may be a need to use optical or microwave manipulation to achieve state selection.

In the remainder of this section, we highlight some recent developments in experimental methodology in the 2020s for producing, trapping and manipulating cold and ultracold molecules.

(a) Laser cooling variants with molecules

The general challenge for the laser cooling of molecules, in comparison to the laser cooling of atoms, is that the method requires a closed optical cycle for the cooling transition, and typically the atom/molecule needs to cycled around this transition 10^3–10^4 times, dissipating energy by spontaneous emission, to bring it to near-zero velocity [7,63]. In molecules, there is a tendency for the excited electronic state to spontaneously emit to a range of different vibration and rotation levels of the ground state, rather than reverting back only to the initial state from which it was excited, and hence the molecules tend to be effectively 'shelved' in the wrong state for the optical cycle, hindering further cooling. The propensity to change the vibrational state on spontaneous emission is determined by the change of geometry of the molecule between the ground and excited state (and the associated Franck Condon factor—the square of the overlap of vibrational wave functions in the ground and excited states). Eventually, the molecule may relax back to the original ground state, but in general, the slow rate of relaxation makes the cooling process highly inefficient or impossible. It is possible, however, to use ancillary lasers to pump the population out of these excited vibrational states to states that will emit back to the ground state in the laser cooling transition. However, depending on the Franck–Condon factors for emission and the rotational selection rules, the number of such pump lasers required may be impractical for a high percentage of molecular species. In general, the rotational states can be controlled by judicious choice of the type of transition—for example, pumping from a lower $J = 1$ level to an upper $J = 0$ level (where J is the rotational quantum number) restricts the transitions that can occur by spontaneous emission (sometimes only back to $J = 1$).

To date, laser cooling has been demonstrated for only a handful of molecules, of which those in the most advanced state of cooling and magneto-optical trapping are the diatomic species CaF [72], SrF [73] and YO [74]. Very recently, the magneto-optical trapping of a triatomic molecule CaOH has been demonstrated [44]—see below. Other molecules under consideration, in some cases with in-principle demonstrations, for laser cooling (or Zeeman Sisyphus cooling—see below) include BaH [75], MgF [76], BaF [77], AlF [78], YbF [79], CH [80], SrOH [81], YbOH [82], $CaOCH_3$ [83] and SrCl [84].

While the majority of species are metal halides, in 2020 McNally *et al.* [75] extended molecular laser cooling to a new class of diatomics, the metal monohydrides, reporting the deflection of BaH molecules. The photon scattering rate (or optical cycling rate) is low for this molecule because of the long lifetime of the upper state, hence they needed to start with a pre-cooled cryogenic buffer gas beam (table 1) as the input to the cooling process. The authors show how their measurements pave the way to the possibility of slowing and trapping such hydride molecules.

The introduction of 'grey-molasses cooling' has recently enhanced these approaches, allowing cooling to lower temperatures than the limit of Doppler laser cooling—in the case of YO, Ding *et al.* [74] demonstrated the cooling to a few microKelvin temperature. They also demonstrated compression of the cloud, which increases the phase-space density. This will allow the loading of such molecules into an optical dipole trap or optical tweezers (see below) and hence a new range of studies.

In 2020, the first demonstration of the laser cooling of a nonlinear polyatomic molecule $CaOCH_3$ to below 1 mK in temperature was made by Mitra *et al.* [83]. The cooling (to 700 μK) was demonstrated along the axis of the beam (in one dimension only)—despite the complexity of the energy level structure of this molecule. Subsequently, in 2022 this Harvard group reported the first 'sub-Doppler' cooling of a polyatomic molecule CaOH, which enabled the Magneto-optical trapping of a polyatomic molecule for the first time [44]. The laser cooling used a principal cooling transition at approximately 626 nm and 11 'repumping' lasers, each at a different frequency, to repump population that had decayed to excited vibrational levels of the ground
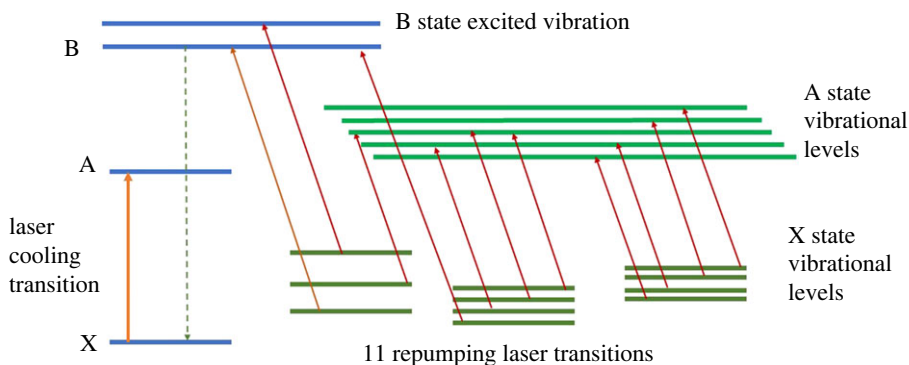
Figure 1. Laser cooling scheme for CaOH, with a principal optical cycling transition at 626 nm. Eleven repumping lasers are required, as indicated, to restore the population to the main cycle following spontaneous decay.

state that were outside the main optical cooling cycle (figure 1). A temperature of $720\,\mu K$ was measured in the magneto-optical trap (MOT), and then a blue-detuned optical molasses (which establishes polarization gradient forces that cool for blue-detuned light and had previously been demonstrated for diatomic molecules) was used to achieve a temperature of $110\,\mu K$. Approximately 20 000 molecules were cooled and trapped in this way. The authors suggest that this technique could be extended to $CaOCH_3$, $SrOCH_3$, $CaSH$, $CaNH_2$ for example, and even 'complex' organic species such as $CaOC_6H_5$.

In 2021, Doyle and co-workers [85] also demonstrated experimentally a variation on the laser cooling methodology—Zeeman Sisyphus cooling—in which they devised a new approach to slow beams of polyatomic molecules to trappable velocities, applied also to the CaOH molecule. By combining a cryogenic buffer gas beam source, which already slows the beam to around $50\,m\,s^{-1}$, with a Zeeman slower with superconducting magnets and optical pumping they were able to slow a significant proportion of those molecules to *ca* $15\,m\,s^{-1}$, which for this molecule is the threshold for trapping in an MOT (although the trapping was not demonstrated in those experiments). The key point is that the Zeeman Sisyphus cooling requires scattering of only a small number of photons (7 in this case, compared to the usual 10^3–10^4 for laser cooling), and therefore the technique is potentially generalizable to a much wider range of molecules. The numbers of molecules emerging from the decelerator per experimental pulse cycle are small, but not so far away from those observed in laser cooling of diatomics. The authors have discussed how this could be increased.

Another exciting recent development is the demonstration that for certain complex species consisting of aromatic ring compounds with a Ba-O or Sr-O group attached to the ring structure, the laser excitation of the electron on the metal atom takes place without disturbing the geometry of the rest of the molecule and hence the Franck Condon factor for the $\Delta v = 0$ transition is large— figure 2 [86,87]. The authors suggest there are possibilities for laser cooling large arene molecules using these transitions. A potential disadvantage of such an approach is that the vibrations of the aromatic ring(s) would not be cooled in the process, but this could possibly be addressed in part by cryogenic helium buffer gas cooling prior to laser cooling.

The extension of methods for laser cooling and trapping of ultracold species into the realm of polyatomic molecules is an important goal for studies of cold chemical systems—and these new results represent a significant step forward. The potential use of complex species brings opportunities to study low-temperature chemistry in more complex chemical systems beyond atom + diatom, or diatom self-reactions—systems where there are multiple reaction paths and product channels; where the complex role of vibration and rotation adds to the fascination of such systems in the quantum regime; where control of orientation and alignment using electromagnetic fields has consequences for chemical behaviour; and where the links to 'real-world chemistry' can be more clearly demonstrated.
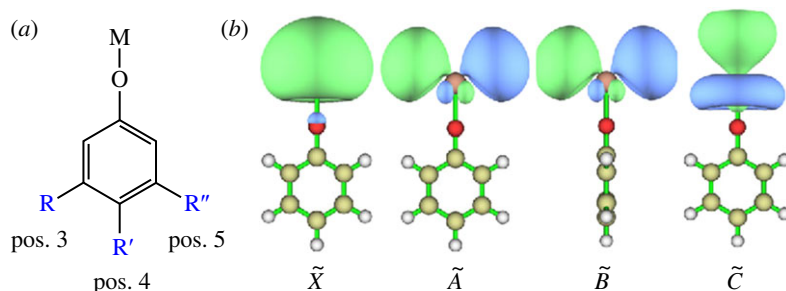
Figure 2. Optical cycling transitions in larger molecules: calculated global minimum structures for $SrOC_6H_5$ illustrate the atom-like character of the electron distribution for the ground (X) and first three (A–C) excited states. The predominant electron density on the metal implies that there is little structural change on excitation. Adapted from [86].

(b) Collisional cooling

(i) Evaporative cooling

In the cooling and trapping of *atoms,* the initial trapping of laser-cooled atoms in an MOT has often been accompanied by the use of evaporative cooling to lower the temperature and increase the phase-space density—driving the system towards quantum degeneracy. In principle, this involves incrementally lowering the trap depth, which allows the more energetic molecules in a sample to escape, followed by thermal re-equilibration and subsequent further lowering of the trap depth. The methodology is dependent on collisions between atoms to re-equilibrate at a lower temperature, and these need to be elastic collisions (or a dominance of elastic collisions) to maintain the atomic quantum states. With molecules, this is more difficult because there tends to be a higher propensity for inelastic collisions (quantum-state-changing collisions). Valtolina *et al.,* in a highly novel approach, created a two-dimensional optical lattice (see §2c) filled with around 20 000 fermionic spin-polarized KRb molecules, and they achieved evaporative cooling through the use of a tunable 'anti-trapping' field to allow the escape of the most energetic molecules from the lattice. This enabled the lowering of the temperature of the ultracold gas below that required for quantum degeneracy (the Fermi temperature) [8]. They used an external electric field to suppress inelastic or reactive collisions (§3a(iii)), thus facilitating the dominance of elastic collisions. The achievement of quantum degeneracy is a key development in the ultracold field and opens the way to the exploration of new and exotic physical/chemical phenomena in such a medium.

An alternative approach to achieving suppression of chemical reactions to enable evaporative cooling is to use 'microwave dressing'. The technique involves creating a repulsive barrier between the molecules by using circularly polarized, blue-detuned microwaves to couple different rotational states of the molecules. This leads to an induced rotating dipole moment, which follows the strong A.C. electric field of the microwaves, and when pairs of molecules approach, the induced moment is aligned and hence the interaction is strongly repulsive. Following earlier studies [88] of the suppression (and enhancement) of inelastic/reactive collisions that was achievable for NaK, Schindewolf *et al.* [89] succeeded in cooling NaK molecules down to 21 nK, well below the Fermi temperature, by using this technique in conjunction with evaporative cooling. High elastic collision rates were observed in the NaK system that were found to exceed the inelastic or reactive ones by at least a factor of 460.

(ii) Sympathetic cooling

It has long been thought that an ideal approach to cooling of molecules would be to cool them sympathetically, via collisions, with an ultracold atomic gas that acts as an ultracold bath. At 'cold' temperatures, cryogenic cooling in a helium buffer gas has been widely used as a

'refrigerant' down to 400 mK and cryogenic molecular beams have been extracted to perform collisional studies, e.g. [17,18,90]. Unfortunately, it has not been easy to achieve molecular cooling using sympathetic cooling at ultracold temperatures because (as with evaporative cooling) this technique requires a dominance of elastic collisions over inelastic or reactive collisions. Nevertheless, this approach may be useful in a small number of systems, and recently Son *et al.* [26] succeeded in cooling LiNa molecules (in a triplet state) through collisions with ultracold Na, taking advantage of a ratio of elastic to inelastic collisions of around 50 for this system. This success was not expected from theoretical predictions. Both species were trapped in a one-dimensional optical lattice settling initially to a temperature of 2.3 µK. By employing two stages of evaporative cooling of the Na atoms, followed by elastic collisional equilibration (i.e. sympathetic cooling), they increased the phase-space density of the molecules by a factor of 20, achieving temperatures of around 220 nK. The preparation of both LiNa and Na species initially in spin-stretched hyperfine states (spin and nuclear magnetic moments aligned) was an important aspect of reducing inelastic collisions.

Hudson's group at UCLA have studied the sympathetic cooling of molecular ions by superimposing an ion trap with an ultracold Rb atomic gas, and reviewed progress in 2016 [27]. For example, they observed that $BaCl^+$ ions could be vibrationally cooled by an ultracold gas of calcium-neutral atoms, with 90% of the $BaCl^+$ reaching the vibrational ground state—one in five collisions leads to vibrational de-excitation. However, the competition of reactive collisions with the cooling collisions is likely to be a hindrance in many other ionic systems, especially as the laser-cooled atoms have a high proportion of excited atoms populated in the laser cooling cycle. This was exemplified by Mohammadi *et al.* [91] who recently studied the evolution of a single $BaRb^+$ ion that was formed and held in a Paul trap and immersed in the 'bath' of an ultracold Rb gas. The molecular ion is initially formed in a weakly bound highly excited vibrational level. They found that the initial evolution is dominated by relaxation to lower vibrational levels, but then other processes become progressively important, including radiative transitions, and atomic ions are observed as products of reaction or photodissociation. It is yet to be demonstrated that vibrational cooling of molecular ions in an ultracold atomic gas is a generally effective approach. In the shorter term, it is likely that cryogenically cooled ion traps (e.g. [92]) will prove to be more versatile in producing vibrationally cold molecular ions, or alternatively the greater use of shaped broadband femtosecond laser pulses to achieve optical pumping of vibrational states towards the ground state [93,94].

(iii) Creating triatomic molecules by magnetoassociation via Feshbach resonances

As highlighted in table 1, one of the most important mechanisms to create ultracold diatomic molecules, is by magnetic field tuning of pairs of ultracold atoms across a Feshbach resonance, in such a way as to lead to association of the two atoms. This method has recently been extended to observe Feshbach resonances of an atom–diatom pair and to find evidence for the creation of triatomic ultracold molecules [95–100]. For example, Yang *et al.* [97] used a radiofrequency pulse to drive association in ultracold mixtures of $^{23}Na^{40}K$ with ^{40}K and reported that a loss feature associated with the association could be observed in the radiofrequency spectra. These authors also observed such trimers directly by radiofrequency-induced dissociation [98]. As with the association of atoms to form diatomics, the triatomics would be formed in very weakly bound states and would need optical pumping (e.g. STIRAP) to reach the ground state. The possibility to associate Rb with CaF has also been considered [100], and the use of Feshbach resonances to suppress or enhance collisions of Na + NaLI studied [99].

(c) Optical tweezers for manipulating single molecules

As indicated in table 1, ultracold molecules can be trapped in a high-intensity region of a red-detuned laser beam by the dipole-force. One approach is to set up an optical lattice, by creating an optical standing-wave field in a cavity with fixed-position intensity maxima in a regular

array. This then creates a two- or three-dimensional lattice of potential energy minima to trap molecules at separations of the order of the optical wavelength employed (figure 11)—ranging from hundreds of nm to a few μm. Examples of applications are given in §3a(iii).

An alternative approach is to use 'optical tweezers' which consist of a tightly focused, translatable laser beam to trap and position single molecules. It has recently been demonstrated that one-dimensional arrays of ultracold molecules can be created and detected by using a line of optical tweezers with each tweezer trapping a single molecule [101]. The demonstration of a two-dimensional array of tweezer-trapped single molecules is on the near-horizon, as has already been demonstrated for atoms [102]. A review article on the trapping and manipulation of atoms and molecules using optical tweezers was published recently [49]. The article also discusses the trapping of alkaline earth atom Rydberg states (e.g. Yb*) for which the state preparation methods can be deployed on the ion core. The creation of arrays of ultracold molecules is important from the point of view of establishing controlled interactions or entanglement for quantum computation (§3b).

Cheuk *et al.* [103] transferred single laser-cooled CaF molecules from an MOT into optical tweezers and succeeded in bringing two such trapped molecules together to study the collisions between the two—see §3a(ii) for further details. Cairncross *et al.* [104] took a different approach—rather than laser cooling a molecule to start with, they assembled two atoms held in a pair of tweezers into a single NaCs molecule that was trapped in an optical tweezer in its internal quantum ground state. They prepared two trapped atoms—one Na atom in a 700 nm wavelength tweezer trap and one Cs atom in a 1064 nm trap—and then cooled these atoms by sideband cooling to the motional ground state. The two traps are merged into a single 1064 nm trap, and then a magnetoassociation experiment (Feshbach resonance association—table 1) is performed to form a weakly bound NaCs molecule (highly vibrationally excited, and also electronically excited). This is then transferred to the ground vibration state by detuned Raman pumping. The overall fidelity of producing the ground-state molecule is about 33% and the lifetime in the trap of the order of 3 s. The lifetime decreases with increasing intensity. In such a trap there are quantized motional states, and these authors report that by first cooling the two atoms to the motional ground state, the molecule itself is also, with 65% probability, in that motional state. The authors sum up by saying that this is *a starting point for parallel molecular assembly in the near future, providing a platform for engineering controlled long-range entangling interactions between molecules. With the addition of microwave and electric field control, molecular qubits for quantum computing applications and simulations that further our understanding of quantum phases of matter are within experimental reach.*

Subsequently, Yichao *et al.* [105] demonstrated a new approach to the association of a pair of atoms (Na and Cs) trapped in a tweezer, using coherent Raman pumping to drive a transition from the unbound pair of colliding atoms to a vibrationally excited bound NaCs molecule with 69% efficiency. This approach obviates the need to have detailed knowledge of the Feshbach resonances used in magnetoassociation, and may broaden the number of chemical species that can be prepared in this way.

(d) Detection and imaging of molecules

Detecting the quantum states of cooled molecules is a critical component of almost any experiment in this field. In a variety of applications of cold or ultracold molecules, it is highly desirable to be able to detect molecular quantum states using methods that do not destroy the molecules. For example, the quantum states of cold-trapped molecular ions have previously been detected by resonant photodissociation techniques [106], but the photodissociation destroys the molecule and hence stops the process being investigated e.g. a chemical reaction or excitation exchange.

Sinhal *et al.* [107] have demonstrated the non-destructive state-selective detection of a cold-trapped molecular ion. In this work, the authors prepared a 'Coulomb crystal' [1] consisting of two trapped ions in a Paul Trap—one ion was laser-cooled Ca^+ and the other was sympathetically cooled N_2^+. The latter was formed in its ground rotational state by

near-threshold photoionization of N_2. The pair of ions is sideband-cooled to the motional ground state of the trap. A one-dimensional standing wave is then introduced (with the laser modulated at the resonant trap frequency) to excite motion, via the optical dipole force, at the resonant frequency of the trap. This motion is only excited when the standing wave frequency is close to the excitation wavelength of a specific transition. They report 99% fidelity of the state-selective detection, and the quantum state is not destroyed (because the laser is off resonant). While N_2^+ is a 'good ion' to work with because of its very long lifetime in a given quantum state and resilience to electric fields, they argue that the methodology could be widely applicable.

In an alternative approach, Drewsen [108] has used optical-comb Raman spectroscopy to drive transitions between THz spaced atomic energy levels—the 3f fine structure splitting of $^{40}Ca^+$, and suggest that this technique could be applied to spin-resolved rovibrational transitions in molecular ions.

Very recently there have been several reports of, or proposals for, using resonant energy transfer between Rydberg atoms and cold/ultracold molecules to selectively and non-destructively read out the quantum states of the ultracold molecules. Patsch et al. [109] considered the case of using rubidium Rydberg atoms to read out the population of ammonia molecules via electric field control of the energy transfer cross-sections. Guttridge et al. [110] demonstrated the blockade of a transition to the 52s Rydberg state in Rubidium in an optical tweezer through the long-range dipolar interaction with RbCs in a specific quantum state, and highlighted the possibility to use Rydberg atoms as intermediates in population transfer between ultracold molecules.

Jamadagni et al. [111] have proposed a novel 'Quantum Zeno-based detection' approach for ultracold polar molecules in an optical lattice, which makes use of the fast chemical reaction between certain molecules such as NaK and one of the atomic constituents (Na in their example). They consider a pair of parallel two-dimensional optical lattice layers, in which one layer is occupied by ultracold atoms and the other is partly occupied by ultracold molecules confined to certain undetermined sites. The aim is to determine which lattice sites are occupied by molecules. Atoms can transfer between one layer and a vacant site in the adjacent layer driven via a Landau–Zener process and this can be detected using 'standard' atomic quantum-gas microscopy techniques. However, if a molecule occupies the site in the adjacent layer, then a fast chemical reaction blockades the atom transfer between lattices and hence no atom is detected at that site. This allows the monitoring of which sites in the optical lattice are occupied by molecules and which are not—a valuable approach to characterizing the molecular occupancy of optical lattices.

(e) Co-trapping

In order to study chemical collisions at very low temperatures (see §3a), it is generally required to be able to cool at least two different chemical species to such temperatures. One of the challenges of such an approach is that those cooling methods are in most cases tailored to specific molecules and therefore different experimental approaches need to be combined—this rapidly escalates the overall experimental requirements.

One approach to studying collisions between different chemical species is to co-trap them for periods long enough to be able to observe collisions at the relevant densities. Karpov et al. [112] have demonstrated the co-trapping of oxygen molecules with carbon atoms paving the way to the study of the important astrophysical reaction $C(^3P) + O_2(^3\Sigma_g^-) \rightarrow CO(^1\Sigma^+) + O(^1D)$ at sub-Kelvin temperatures. They entrained carbon atoms, produced by laser ablation, into a supersonic beam of O_2 and then passed these into a moving-trap Zeeman decelerator, capable of co-trapping both species—the trap depth was 0.6 K for carbon, and 0.8 K for oxygen—with a mean velocity of $375\,m\,s^{-1}$ in the Kr carrier gas. The beam is then decelerated and trapped by a superconducting magnetic trap (figure 3). The C atoms are detected by resonance-enhanced multiphoton ionization (REMPI) as a function of delay from the initial trapping time, with a translational temperature of order 1K. They estimate densities of carbon at $10^7\,cm^{-3}$, and O_2 at $10^{10}\,cm^{-3}$. In the presence of co-trapped O_2, the decay rate of the carbon atom population increases by a factor of 5 attributed
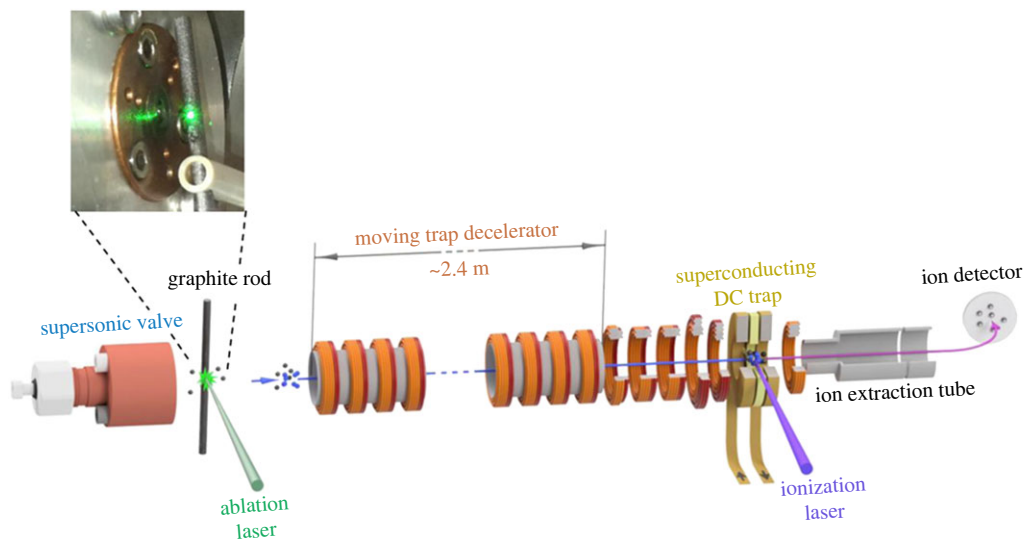
Figure 3. Zeeman moving-trap decelerator apparatus for co-trapping reactive cold paramagnetic atoms and molecules—in this case, carbon atoms and oxygen molecules. Adapted from [112].

to the above reaction. Currently, the products of the reaction have not been detected (only the reactant decay), which would in any case be difficult as the products rapidly leave the trap in this exothermic chemical process. It is also not clear how the temperature could be varied in these experiments, but they point out the possibility to do studies with isotopomers of O_2, e.g. $^{16}O_2$, $^{18}O_2$, $^{16\,18}O_2$.

Jurgilas *et al.* [46] studied collisions of CaF with Rb in a dual-species magneto-optical trap at 2.4 mK. CaF molecules were prepared by laser cooling (with three vibrational repump lasers) of a CaF beam—generated from a cryogenic buffer gas source and slowed to low velocity using a frequency-chirped counter-propagating laser beam, and then captured into the MOT, which was also set up to trap ultracold Rb atoms. The CaF molecules occupied both the $v = 0$ and $v = 1$ vibrational levels as the laser cooling scheme operates on both states that are populated under the experimental conditions. The set up involved one MOT but two sets of six cooling laser beams overlapped. Typically, they load from 9×10^8 to 8×10^9 Rb atoms and 10^4 CaF molecules. By observing fluorescence from the molecular cloud as function of time, the decay of the trapped molecules was monitored. For the CaF–Rb collisional loss process they determined a rate constant $k_2 = (1.43 \pm 0.29) \times 10^{-10}\,\mathrm{cm}^3\,\mathrm{s}^{-1}$, and were able to separate out contributions to the rate from the ground and excited states of Rb, which are both populated in the laser cooling process. They found that capture theory [2,68,113] provides an appropriate description for the scattering rate, and they attributed the loss to rotational inelastic processes, rather than chemical reaction.

Fitch *et al.* [48] also demonstrated a dual-trap that used static magnetic fields to trap ultracold Rb atoms and electrostatic fields to trap ammonia NH_3 molecules, which were fed into the trap from a Stark decelerator (table 1). This trap was then used to study cold collisions between Rb and NH_3 (and ND_3). They observed the decay of ammonia density in the trap, detected using a REMPI technique, and found a significantly faster decay when Rb is present. This is attributed to inelastic collisions and the authors discuss and simulate some of the complications in this experiment, such as the impact of the inhomogeneous electric fields on the scattering cross-sections and the varying collision energy across the trap volume.

While this section has focused on the co-trapping of species that are produced from a different source, or are chemically very different, there have been a wealth of studies involving the co-trapping of alkali metal diatomic species with the ultracold atoms that they were produced from.

Figure 4. 4.5 m length Stark decelerator at Gronigen designed to produce slow beams of heavy diatomic molecules for studying fundamental symmetry violations. Adapted from [114].

For example, in trapped mixtures of ^{23}Na atoms and ^{23}Na^{6}Li molecules, Son *et al.* [99] measured reactive collisions, NaLi + Na $\rightarrow$ Li + Na$_2$, and were able to control the rates of the collisions by a factor of over 100 using magnetic field tuning across a Feshbach resonance.

These experiments illustrate that the co-trapping of different chemical species in a trap in the ultracold, or low-end of the cold temperature range, is now possible for selected examples and this offers promise for future chemical studies. However, it must also be recognized that each of these examples involves one molecular and one atomic species, and the co-trapping of two different molecular species is much more challenging and yet to be implemented.

(f) Stark and Zeeman deceleration

The Stark decelerator was one of the earliest of the 'new devices' developed in the late 1990s and early 2000s to produce cold samples of polar molecules with well-controlled velocities [11]. However, its use has been confined largely to relatively light species to date, for example, NH$_3$, OH, CH$_3$F and CO. This is because the number of high-voltage pulsed-deceleration stages required increases in proportion to molecular mass, and the hundreds of stages required for heavy molecules leads to significant transmission losses, and other experimental issues. In addition, the Stark effect becomes quite nonlinear for the lowest rotational states of heavy molecules meaning the deceleration is less efficient.

Using a 4.5 m long travelling-wave (moving trap) Stark decelerator—figure 4—Aggarwal *et al.* [115] have demonstrated the possibility to decelerate SrF molecules and to trap them for up to 50 ms with a kinetic-energy spread of 60 mK. In this case, the molecules were loaded into the Stark decelerator from a cryogenic buffer gas beam source (table 1) in order to start with a fairly low velocity before deceleration. The significance of this outcome is in the achievement of deceleration to a mean velocity of zero of a 'heavy molecule' [114]. In the context of fundamental physics measurements (see §3c) this is an important development, because such molecules have a highly increased sensitivity to measure potential deviations from predictions of the 'standard model' of particle physics.

An approach to decelerating non-polar species using the extremely large dipole moments that could be generated on excitation of the atoms or molecules to high Rydberg states was first demonstrated by Procter *et al.* [14]. Since then, sophisticated designs of miniature chip-based decelerators have been developed and electrostatic trapping implemented and have been deployed in a range of scattering experiments [116,117]—see §3a for more details.

There have also been significant recent developments in the design and use of the Zeeman decelerators and magnetic guides. For example, Mohamed *et al.* [118] have demonstrated the benefits of using evolutionary algorithms to optimize the throughput and purity of Zeeman decelerated and guided H-atom beams. Cremers *et al.* [119] have developed a Zeeman decelerator with 100 pulsed solenoids alternating with 100 permanent magnet-focusing elements, which is optimized for use in crossed-beam experiments. The application to study highly angularly resolved scattering of carbon and helium atoms demonstrated the value of this device [120] and provided a stern test for quantum scattering theories. Damjanović *et al.* have demonstrated the performance of a new type of travelling-wave Zeeman decelerator, decelerating OH molecules from a velocity of 450 to 350 m/s. The design enables a full three-dimensional confinement of the molecules and hence significant improvements in phase-space acceptance, ultimately leading to more intense, and better-controlled beams of decelerated molecules [121]. An application in the use of a travelling-wave Zeeman decelerator to co-trap two paramagnetic species [112] has been described in §2e (see also figure 3).

3. Recent applications of cold and ultracold molecules

In this section, some new applications of the technologies developed to produce, manipulate and detect cold and ultracold molecules are described, including cold and ultracold chemistry, astrophysical chemistry, quantum computation, condensed matter physics and fundamental physics. Perhaps, the greatest progress to date has been with applications in the cold and ultracold chemistry area, and this is reflected in the emphasis of this section.

(a) Cold and ultracold chemistry

The study of cold and ultracold chemical reactions is often targeted at the direct observation of quantum effects in chemical reactions, which are expected to become very prominent at low temperatures [60]. These include the effects of internal quantum state populations (e.g. vibration, rotation, hyperfine states) on the reactivity; the observation of quantum tunnelling through low-energy barriers or quantum reflection at the edge of a potential energy drop on the approach of reactants; the observation of resonances in the reaction cross-section versus energy plot; the observation of long or unexpected lifetimes of the intermediate reaction complexes; non-adiabatic effects on reaction rates due to state-transfer (mixing) between close-lying potential energy surfaces in the course of the reaction; strong effects of electric and/or magnetic fields on reactivity or the use of microwave fields to control outcomes; effects of single partial-wave collisional behaviour (see below) and ultimately coherent effects under conditions of quantum degeneracy.

(i) Cold chemistry ($T > 1$ mK)

In the cold temperature range, a number of recent experiments have taken advantage of the low-relative-velocity collisions achievable when a pair of supersonic molecular beams, with species in the two beams travelling at a very similar velocity, are either merged into a single beam or crossed at a narrow angle, e.g. 10° (table 1). The value of such approaches was already demonstrated in the early 2010s [38,122,123] for Penning ionization reactions (e.g. $He^* + H_2 \rightarrow H_2^+ + He + e^-$, where He* is metastable helium in one of the triplet $n = 2$ states) and radical reactions (e.g. $S + H_2 \rightarrow SH + H$). The collision energy resolution is particularly high in the merged beam approach, and has enabled the observation of narrow resonances in the reaction cross-section at specific collision energies for the Penning ionization reaction down to a few milliKelvin in temperature.

The observation of resonances in the reaction cross-section—peaks in the reaction probability as a function of collision energy, which may be considered to be located at the energies of the quantized states of the collisional complex—is a key indicator of the quantum effects coming to
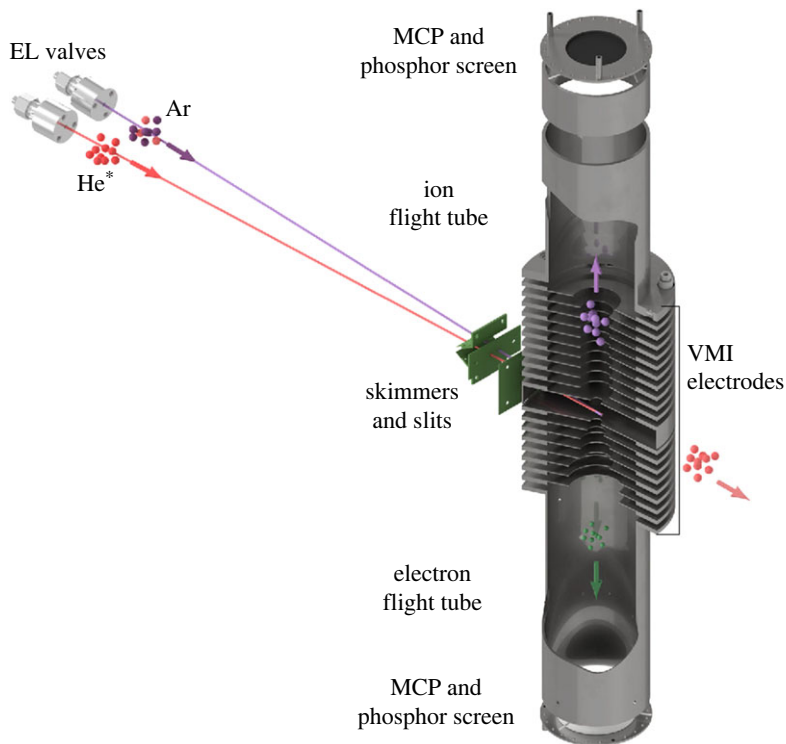
Figure 5. Merged beam experiment for studying low-energy collisions between helium metastable atoms and rare gas target species. The paramagnetic atoms in the metastable helium beam are deflected into the path of the target beam (Ar in this case). The apparatus has been extended to incorporate co-incident detection of electrons and ions produced in single Penning ionization events, using velocity-map imaging. The setup enables both angular and energy measurements on the ions and electrons. Adapted from [124].

the fore at low temperatures. In classical dynamics, every individual collision between a pair of molecules (or particles more generally) will have a specific collisional orbital angular momentum ℓ—which has zero magnitude for a head-on collision and is large for a glancing collision. At low collision energies (low T), we need to consider the quantization of ℓ. A quantum mechanical collision is described in terms of incoming and outgoing waves, which are expanded as a sum of 'partial waves', each with a particular integer value of the orbital quantum number ℓ. Resonance effects in the collision will only be observed if a small number of partial waves contribute to the collision. This is not the case at room temperature, but the number of partial waves reduces with the temperature and ultimately a single partial wave ($\ell = 0$) may be a sufficient and complete description of the collision at ultracold temperatures. It is particularly in the few-partial-wave regime where resonances have been observed.

In 2020, Margulis *et al.* [124] extended the capabilities of the pioneering merged beam Penning ionization experiments at Weizmann Institute by adding the facility to measure the energy and angular distributions of the post-reaction trajectories of both the ions and the electrons that are produced in their experiments (figure 5). They were able to detect pairs of electrons and ions in co-incidence (i.e. arising from the same collision event). Applying this initially to $He^* + Ar \rightarrow [HeAr^+]^* + e^- \rightarrow He + Ar^+ + e^-$, the electron energy distribution gives information on the quantum state of short-lived ionic complex $[HeAr^+]^*$ that is formed as the intermediate in the reaction. The angular distribution of the ions is indicative of the angular momentum components of the resonant state of the complex that is formed, while the kinetic-energy distribution of the ions indicates their quantum state distribution (spin-orbit states in this case).

From the same group, Paliwal *et al.* [125] observed the non-reactive elastic (non-state-changing) and inelastic (state-changing) scattering of metastable helium atoms with deuterium molecules. As in the previous Penning ionization experiments from this group, in which very high collision-energy resolution in the milliKelvin effective temperature range was achieved, a series of resonances was observed at specific collision energies in the elastic and inelastic cross-sections. They measured the angular distribution of the metastable helium atoms (using near-threshold ionization of these atoms at 260 nm to produce the detected ions) that were scattered by elastic collisions in the range of 0.5−50 K, and compared this data with previous measurements of Penning ionization in the same system ($He^* + D_2 \rightarrow D_2^+ + He + e^-$). Additional resonances were observed in the same energy range as Penning ionization, and by comparison with quantum scattering calculations and analysing the partial-wave cross-sections, they could distinguish between two types of resonance that occur in these collisions—the shape resonance, where the collisional state is trapped behind a centrifugal barrier, and the orbiting resonance which is a state that is less localized and can exist above the barrier.

Tanteri *et al.* developed a related methodology to studying chemi-ionization reactions in a merged beam experiment. By determining the distribution of electron kinetic energies using velocity-map imaging they were able to estimate a branching ratio between associative ionization and Penning ionization ($A^* + B$ forming $AB^+ + e^-$ or $A + B^+ + e^-$, respectively) [126].

Merkt and co-workers [39,127] have applied a pioneering merged Rydberg beam + molecular beam approach to study a number of ion–molecule reactions in the range from 10s of Kelvin down to around 10 mK, a technique first demonstrated in 2016. While the merged beam approaches described above have enabled the measurement of a select handful of neutral–neutral reactions at temperatures down to a few milliKelvin with high collision energy resolution, such methods cannot be so easily applied directly to ion–neutral reactions. The problem is that the charge of the ions leads to collision-energy broadening through the effect of small stray fields and space-charge effects (many ions in a small volume). These space-charge effects can be eliminated by using Rydberg states of the corresponding neutral molecule/atom instead of ions; for example, using $H_2(n)$ or $He(n)$ Rydberg states (where n is a high principal quantum number) instead of H_2^+ or He^+ ions. At principal quantum numbers of the order of 30, the Rydberg electron orbital is so diffuse that the Rydberg electron acts as a spectator in the collision [128], and the neutral molecular ground state species collides with the ionic core of the Rydberg species. This is effectively an ion–neutral collision, with the benefit that the Rydberg species is charge-neutral overall and thus is not subject to collision-energy broadening, enabling high-resolution collision energy measurements in a novel merged beam experiment (figure 6).

For the $H_2 + H_2(n)$ system studied, equivalent to the astrophysically important reaction $H_2 + H_2^+ \rightarrow H_3^+ + H$, the measurements were made down to collision energies of a few milliKelvin, and with multiple isotopic variants (HD, D_2, H_2^+ HD^+). The comparison of H_2 reactions with D_2 reactions revealed a difference in the chemical reactivity of the neutral molecule in its $J = 0$ state (slower) compared to $J = 1$ (faster). This difference was attributed to the fact that the attractive interaction of the molecular quadrupole moment of the H_2 with the ion only has a positive effect on the reaction rate in the $J = 1$ state, not $J = 0$, and even for $J = 1$ this effect only becomes apparent at the lowest temperatures. The measurements provided a clear indicator of reactant quantum-state-specific effects at low temperatures [127]. They also adapted the experiment to be able to observe different ionic products by mass-spectrometry using a two-pulse extraction scheme. Analysing the time-of-flight distributions of the H_3^+ and H_2D^+ products from the reaction of $H_2(n) + HD$ gave information on the kinetic-energy distribution of the product ions and allowed the determination branching ratios of the $H_3^+ + D$ and $H_2D^+ + H$ reaction channels [129]. The reaction was studied at collision energies E_{coll} between 0 and 30 K with a resolution of about 75 mK at the lowest energy measured. Seven per cent of the available energy was found to be released as kinetic energy, and the branching ratio into the $H_3^+ + D$ product (as opposed to $H_2D^+ + H$) was measured to be 0.225(20), i.e. the D atom of HD was more likely to transfer to the molecular product than the H atom. This branching ratio (and others in
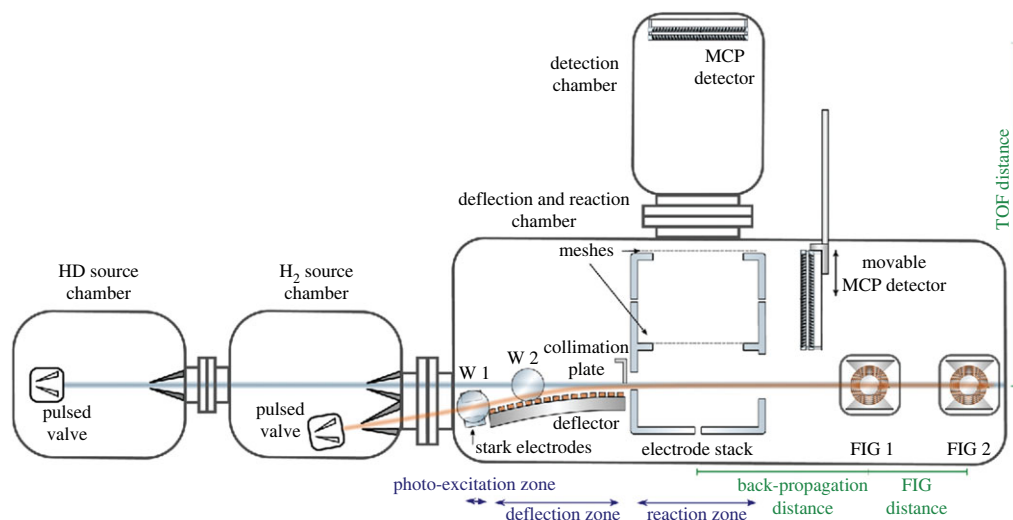
Figure 6. ETH Zurich experiment to merge a beam of Rydberg molecules (or atoms) with a ground state neutral molecule beam to study the collision energy dependence of low-energy ion–molecule reactions. The curved surface-mounted deflector guides the Rydberg beam into the path of the other beam and controls the relative velocity. Reactions occur within the Rydberg electron orbit (see text) and the ionic products of these shielded ion–molecule collisions are detected with high mass resolution. Adapted from [129].

the various combinations of isotopomeric reactants) suggests that the branching is driven by the higher density of states in the deuterated product molecule H_2D^+.

The observed collision energies for the $H_2^+ + H_2$ system are approaching the predicted transition to pure quantum behaviour—pure s-wave scattering—expected to occur for this very light (low-mass) system at around 1 mK, and the most recent measurements on $H_2^+ + para -H_2$ ($J = 0$) show evidence for a marked increase in the cross-section at the lowest collision energies, as predicted for the contribution from s-wave scattering [130].

In a series of recent papers, the Merkt group has also reported on the reactions of $N_2 + He(n)$, $CH_4/CD_4 + He(n)$, $NH_3/ND_3 + He(n)$ and $CH_3F + He(n)$ (where He(n) indicates a helium atom in a Rydberg state of high principal quantum number n) [131–134]. Their study of the $NH_3 + He(n)$ reaction [133]—which should quantitatively follow the rate of the charge transfer process $NH_3 + He^+ \rightarrow NH_3^+ + He$—revealed a very interesting inverse isotope effect (faster reaction of ND_3 compared to NH_3). In their analysis, they extended existing rotationally adiabatic capture theory calculations to include the effects of hyperfine structure and nuclear-spin statistics, and were able to describe how the nuclear-spin statistics—the population of rotational levels and the different reactivity of those rotational levels—explained the observed isotope effect.

The rate of reaction of CH_3F with He^+ showed a strong enhancement at temperatures below 1 K, and using a rotationally adiabatic theoretical model the authors concluded that this was a consequence of the alignment of the CH_3F dipole to the collision axis in a specific quantum state $J = 1$, $KM = 1$ [134]. For the other species colliding with He(n), alignment effects due to the negative quadrupole of N_2 were observed, while, in contrast, for CH_4 the lowest order multipole moment of CH_4—the octupole—was calculated to have little impact on the overall rate constant at these temperatures. However, the isotope effect for the CH_4/CD_4 species could not be fully explained using adiabatic capture models [132]. Overall this series of results illustrates the detailed understanding of the factors that govern low-temperature chemistry that can be gained through cutting-edge experimental methods in combination with theory.

In a low-angle (10°) crossed-beam experiment, Van de Meerakker and co-workers studied *inelastic* collisions of NO molecules with He atoms [135] and with H_2 molecules [136], which
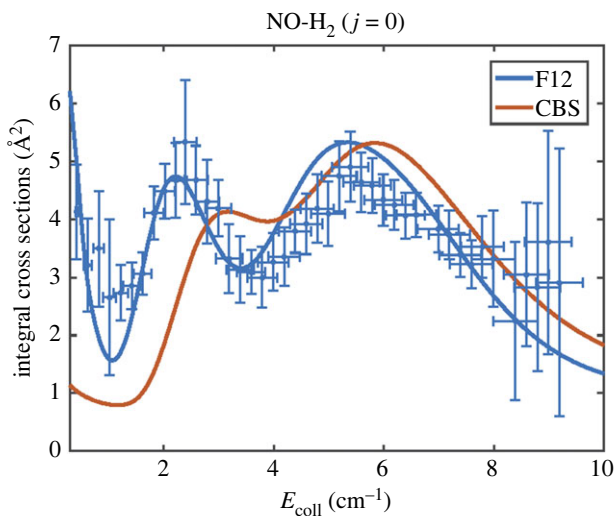
Figure 7. Collision energy dependence of the integral cross-section for inelastic scattering of NO with H_2 illustrating the comparison of the experimental cross-section with calculated cross-sections based on potentials (F12 and CBS) differing by a well depth of only 2 cm^{-1}. Adapted from [136].

resulted in a collision-induced change between NO rotational levels of different parity but the same total angular momentum J. The collision energies employed were in the range 0.4–10 cm^{-1} (equivalent to a temperature down to *ca* 300 mK), using a combination of a Stark decelerator, crossing a cryogenically cooled He or H_2 beam at a 10° angle. The velocity-map-imaging technique was used to detect the angular distribution of inelastically scattered NO molecules (the differential cross-section). In both cases, these quantum-state-changing collisions show resonances in the integral (ICS) and differential (DCS) cross-sections revealing details of the quantum states of the collision complex and reflecting the partial-wave behaviour in the collisions. In particular, at resonance energies, the number of nodes in the DCS is a direct indicator of the partial-wave character of the complex. In order to reproduce these resonances in theory, an extremely high level of *ab initio* calculation of the NO–He or NO–H_2 potential energy surface is required. The CCSDT(Q) method gave accurate predictions for NO + He but a calculation at this level was too difficult for NO + H_2. The comparison of results with calculations from two different CCSDT potentials for NO + H_2 showed the results were sensitive to differences in the calculated short-range well depth as small as 2 cm^{-1} (figure 7). Such studies have recently been extended to C + He inelastic scattering [120].

Using a very different technique, Koller *et al.* [137] have used a combination of a buffer gas-cooled beam and a centrifuge decelerator to trap CH_3F molecules and study $CH_3F + CH_3F$ collisions at temperatures of *ca* 400 mK (figure 8). While the loss of CH_3F from the trap was found to occur at the rate expected for dipole–dipole inelastic collisions, and there is no self-reaction, the method may be applicable to studying low-energy collisions of more complex polar species in selected cases where the sufficient density of cold molecules can be achieved.

With a different emphasis, but moving to more complex chemical systems, Kilaj *et al.* [138] demonstrated how the techniques of cold-molecule science could be applied to bring insights into the mechanism of a chemical reaction type of mainstream interest—the Diels Alder reaction. Using an electrostatic deflector (a variant on the quadrupole velocity selector—table 1) they were able to spatially separate the two conformers of dibromobutadiene (s-trans and gauche) and study the reaction with propene ions that were sympathetically cooled into a laser-cooled Ca^+ Coulomb crystal. This reaction is a cyclo-addition reaction (figure 9), and there has been discussion over many years in the literature about the extent to which the bond-making process is synchronous or stepwise across the two bonds.
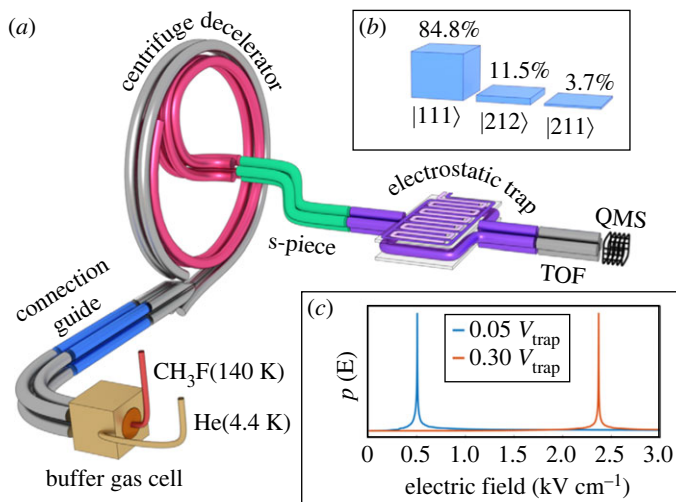
Figure 8. (*a*) Centrifuge decelerator experiment to observe self-collisions of CH$_3$F molecules, which are first cooled in a buffer gas cell, then extracted into a quadrupole guide, decelerated using the centrifuge device and trapped in a surface-mounted electrostatic trap. (*b*) Rotational population distribution in the trap $|\mathrm{JKM}\rangle$ and (*c*) electric field distribution of the electrostatic trap. Adapted from [137].
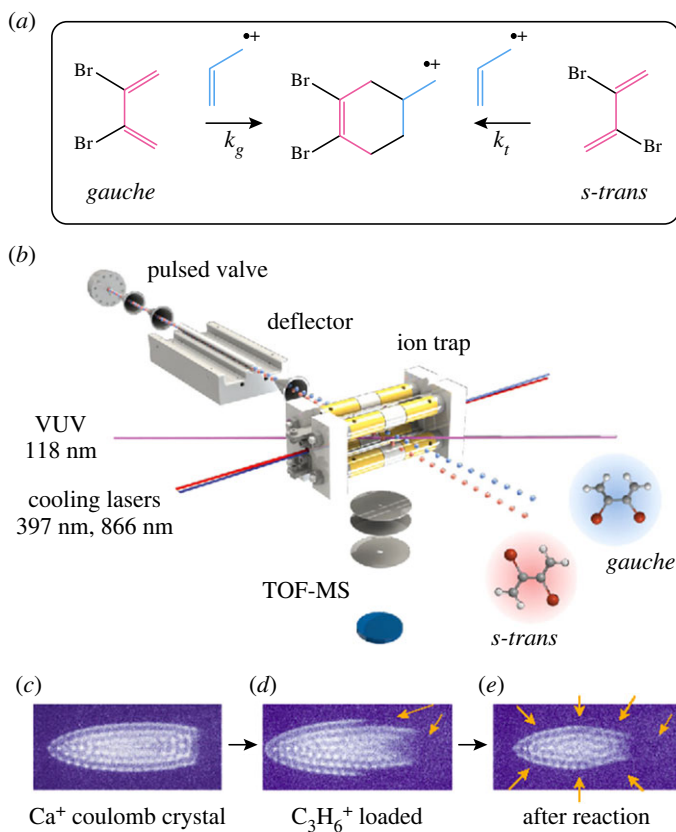

Figure 9. Experiment to measure a classic Diels–Alder reaction between two conformers of dibromobutadiene and propene ions. As illustrated in (*b*) the conformers have a different trajectory across the deflector, hence the deflector can be tilted to send either conformer (predominantly) into the laser-cooled ion trap. Adapted from [138].

Somewhat surprisingly in this example, it was found both conformers reacted at 'capture-theory predicted rate' (see e.g. [113])—i.e. both reactions were very fast despite the fact that only one of the two conformers (gauche) has the geometry required for the expected concerted mechanism of the cyclo-addition. Detailed *ab initio* calculations of the reaction pathway provide an explanation suggesting that this system was at the borderline between 'concerted' (two bonds formed simultaneously) and 'stepwise' (one bond at a time) [138].

(ii) Cold reactions and astrophysical relevance

One of the key challenges in interstellar chemistry is to understand the origin of the so-called 'deuterium fractionation' problem [139,140]. In brief, the relative abundance of deuterated molecules such as ND_3 detected in the interstellar gas phase (as compared to non-deuterated molecules) far exceeds the predictions based on the relative abundance of elemental deuterium (versus hydrogen) in the universe. This suggests that either there are mechanisms for incorporating deuterium into molecules which have faster rates than the corresponding hydrogen species, or that the deuterated molecules are somehow more resistant to reverting back to the elemental form.

Molecular and atomic ions have been identified as key constituents of interstellar gas clouds [2], their abundance reflecting the lack of protection from ionizing radiation present in space. The observation of H versus D isotope effects in cold ion–molecule reactions is, therefore, of interest to the Deuterium Fractionation problem. Using laser-cooled, trapped ions in a Coulomb crystal, Petralia *et al.* [141] observed a very large 'inverse isotope effect' for the charge transfer reaction of Xe^+ with NH_3/ND_3—the ND_3 reacts faster by a factor of 3. This unusual phenomenon was attributed to the greater propensity for the intermediate complex $[NH_3–Xe]^+$, formed when the Xe^+ and NH_3 come together as an intermediate in the reaction, to revert back to the reactants in the NH_3 case (rather than proceeding to the charge transfer), and the intrinsic slowness of the charge transfer in both cases. In essence, the ND_3 molecule has more time available to enact the slow electron transfer within the $[ND_3–Xe]^+$ complex than the NH_3 has in the equivalent complex, because the deuterated complex is more stabilized against dissociation by intramolecular energy transfer. While Xe^+ is not itself a major constituent of interstellar media, the authors point to the possibility that this could be relevant to other ion–molecule collisions in which a charge transfer step is relatively unfavourable. It was also found that the inverse isotope effect increases on going down the periodic group Ar^+, Kr^+ and Xe^+ [142]. For argon and krypton, it is believed that the charge transfer step is faster and less dependent on the isotopic differences. A discussion of the role of long-lived complexes at *ultracold* temperatures is provided in §3a(iii).

The modelling of the abundances of molecules in the interstellar medium (ISM) is reliant on accurate rates of reactions at interstellar temperatures (roughly 10–50 K) and on the branching ratios into the alternative products that might be formed. Even though ion–neutral molecule reactions are a major constituent of interstellar chemistry, the rates of many such reactions have not been measured in the laboratory at low temperatures. Lewandowski and co-workers have used a laser-cooled ion-trap coupled with high-resolution time-of-flight product analysis (see also [143]) to observe a series of reactions of relevance to the astrophysical medium. For example, the reaction of CCl^+ with benzene is found to produce carbocations $C_7H_5^+$, $C_5H_3^+$ and $C_3H_3^+$ providing insights into potential pathways to larger carbocations in the ISM [144].

Hudson and co-workers [145] have used a combination of a laser-cooled ion trap with a cryogenic buffer gas beam, also with time-of-flight mass spectrometric analysis, to study important astrophysical reactions such as $C^+ + H_2O$ at the temperature of interstellar gas clouds. In this case, the branching ratio for producing either HCO^+ or HOC^+ was obtained, and the mechanism is an important one for forming the metastable HCO^+ ion in the ISM. They were able to understand the predominant formation of HOC^+ by comparison with quasi-classical trajectory (QCT) calculations on a six-dimensional potential energy surface.

Negative-ion reactions have also been studied to low temperatures in cryogenic ion traps, and Wild *et al.* [146] have reported the measurement of the rate of the proton-transfer tunnelling reaction of hydrogen molecules with deuterium anions $H_2 + D^- \rightarrow H^- + HD$. The measured rate constant $(5.2 \pm 1.6) \times 10^{-20}$ cm^3 s^{-1} is 10–11 orders of magnitude lower than typical ion–molecule reaction rates (the authors note that this is the lowest measured bimolecular ion–molecule reaction rate constant by four orders of magnitude); and this observation, at temperatures down to a collision energy of 15 K, is a testament to the very high sensitivity and long ion storage time of the 22-pole ion trap measurements. The measured rate is in good agreement with quantum scattering predictions, for this most-fundamental example of all ion–molecule reactions.

(iii) Ultracold chemistry

In the ultracold regime, a number of highly novel experiments have been carried out recently using optically trapped molecules, including experiments with single molecules confined in the tight dipole trap of an optical tweezer, or alternatively experiments with molecules in two- or three-dimensional array of optical traps, created by a standing wave laser field (figure 11). Such experiments bring a new level of control over the reaction parameters. However, the relatively shallow depth of optical traps (typically less than 10 mK) means that these experiments can only be performed in the ultracold region.

In a remarkable series of experiments, Ni and co-workers [67,147] studied the full dynamics of the bimolecular reaction, $KRb + KRb \rightarrow [K_2Rb_2]^* \rightarrow K_2 + Rb_2$, where $[K_2Rb_2]^*$ represents an intermediate complex formed (figure 10) at temperatures around 500 nK. KRb molecules were prepared in the absolute internal ground state (the lowest rotational and hyperfine state) at this temperature by magnetoassociation of laser-cooled atoms and optical pumping to the ground state using stimulated Raman adiabatic passage (STIRAP). Approximately 5000 molecules were held in a crossed-beam optical trap (1064 nm wavelength beams) and the self-reaction of KRb, a reaction that is almost thermoneutral, was studied.

In this work, they used spectroscopic techniques—REMPI—to characterize the rotational quantum state distributions of the product species, K_2 and Rb_2 generated in the reaction. They observed that the nuclear spin of each atom was conserved in the passage from reactants through to products—thus for example if the initial state of the colliding KRb molecules all had oppositely aligned nuclear spins, K↑Rb↓, then the final states of the product molecules were K↑K↑ and Rb↓Rb↓ [148]. This confirmed general predictions using symmetry rules about nuclear spin conservation in reactions that had been made many decades earlier, e.g. [149]. They were also able to observe the correlation in single collisional events between the rotational states of the K_2 product molecules and the rotational states of the Rb_2, and test whether these were statistically distributed—some deviations observed were attributed to the specific partial-wave character of the outgoing wave describing the separation of products.

In addition, an ultraviolet laser was used to ionize the intermediate complex ($K_2Rb_2^*$) with mass selective detection, and its lifetime could be measured through delaying the time between creation and detection. Among the most interesting observations of their work was the very long lifetime that was measured for this complex—around 360 ns, which is many orders of magnitude greater than lifetimes of reaction complexes observed at 'normal temperatures', but within the reasonable agreement—a factor of 2—of predictions of statistical theories such as RRKM theory based on high-quality *ab initio* density-of-states calculations. In the field, there remains some controversy about the lifetimes of complexes observed across several molecular alkali-metal dimer collision systems, which in some cases are orders of magnitude above RRKM predictions [67,150,151]. The role of photoexcitation of the intermediate complex by the optical trapping lasers has been demonstrated to be significant in some cases, including the KRb + KRb system, complicating the interpretation of complex lifetimes. To evaluate this effect, Ni and co-workers were able to abruptly reduce the intensity of the 1064 nm trapping laser while measuring the lifetime, to separate the effect of the trapping field on the lifetime from the intrinsic lifetime
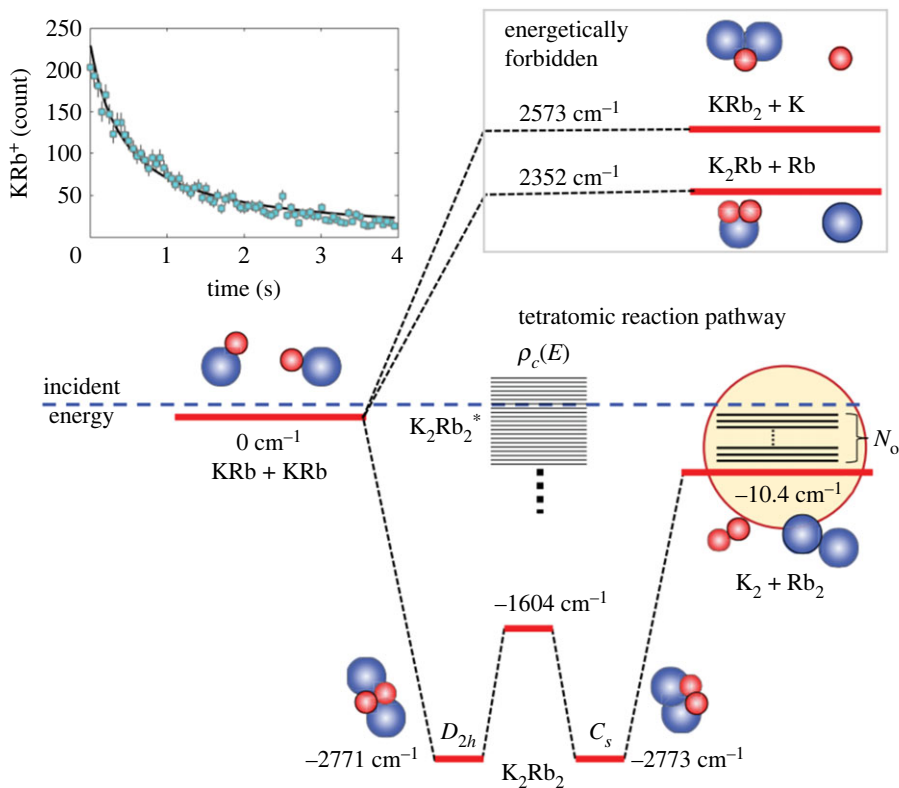
Figure 10. Reaction energetics for the ultracold reaction between pairs of KRb molecules. Adapted from [60].

(360 ns) [152]. Likewise, Gregory *et al.* [153] reported similar measurements using modulation of the trapping field to find a much longer lifetime (530 µs) for the RbCs + RbCs complex, a non-reactive system. The three orders of magnitude difference to the KRb system is explicable through the much higher density of states in the heavier [RbCs]$_2$ complex molecule. In this case, the long intrinsic lifetime of the complex provides an explanation for the susceptibility to losses by photoexcitation of the complex.

Following their early studies on chemical reactions between aligned molecules in an optical lattice [154], in 2022, Ye and co-workers [155] reported a remarkable study on reactions between 'layer-resolved molecules' in a three-dimensional optical lattice. By applying an inhomogeneous electric field to a stack of two-dimensional lattice layers, they shifted the microwave spectroscopic transition frequencies differentially for each layer, and could use this to independently control the rotational quantum states of each of the two-dimensional layers of KRb molecules (see e.g. figure 11). They demonstrated that the reaction rate of molecules in one layer was affected by the rotational quantum states of the molecules in the adjacent layers. In this system, it had previously been demonstrated [154] that indistinguishable molecules (in the same quantum state) react slowly in a layered lattice—the reaction is suppressed—whereas molecules in different quantum states react much faster. This is technically because the faster reacting s-wave type collisional process is allowed for 'distinguishable' pairs of molecules, but not for 'indistinguishable' ones. Thus, if all the molecules in a given layer are in the same quantum state, e.g. $|0\rangle$, the reaction rate is relatively slow. If the adjacent layer contains molecules in the state $|1\rangle$, then through a dipole-induced interaction there may be state-exchange between pairs of molecules, creating an interloper molecule in the $|0\rangle$ layer in state $|1\rangle$, and there is then rapid loss of this molecule through the chemical reaction of a distinguishable pair.

The use of optical tweezers in reaction studies is now coming into prominence in studies of ultracold molecular collisions. In a landmark study, Cheuk *et al.* [103] observed collisions
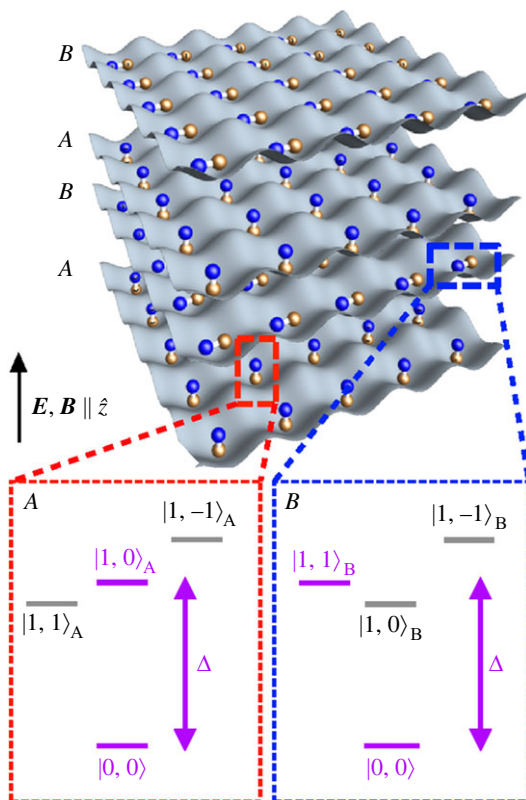
Figure 11. A two-dimensional optical lattice array, indicating how single molecules or atoms can occupy a potential energy minimum in the interaction profile between the molecule and the off-resonant electromagnetic standing wave field. Adapted from [156].

between a pair of isolated ultracold molecules, each held in an optical tweezer. The individual CaF molecules in these experiments were brought to a temperature in the microKelvin range by laser cooling and trapped in an MOT. A sample of these cold molecules was then transferred to a one-dimensional optical trap, and this was then used to load a pair of optical tweezers in such a way that just one CaF molecule was held in each of the tweezers. After optical/microwave preparation of the two molecules in a specific rotational and hyperfine state, the two optical traps were merged into one trap (by moving one trap using an acousto-optical deflector into the space of the other and switching that trap off) and then these molecules were allowed to interact for a period of time. After that time, the molecules were separated again into a pair of tweezers (if they had not been lost through collision) and detected (illustrated in figure 12*a*). The 'two-body loss rate' was measured by observing the survival probability of two molecules as a function of time spent in the merged trap. These authors interpreted the loss rate as being consistent with either a chemical reaction ($CaF + CaF \rightarrow CaF_2 + Ca$), or with the formation of a long-lived association complex. The temperature of the collisional pairs was estimated to be 41 µK, which is below the threshold for pure s-wave behaviour and therefore in the 'full quantum regime'. As methods for laser cooling of molecules continue to develop, there are prospects here for studying a wide variety of collisions at a single-particle level.

Subsequently, Anderegg *et al.* [158] studied the suppression of reaction between pairs of CaF molecules held in an optical tweezer using the microwave dressing approach (see also §2b(i))). They showed that tuning the microwave frequency from blue to red detuned, changes the inelastic collision rate by a factor of 24, as the system changes from being shielded from short-range collisions to being 'anti-shielded' (enhanced short-range collisions). The potential for
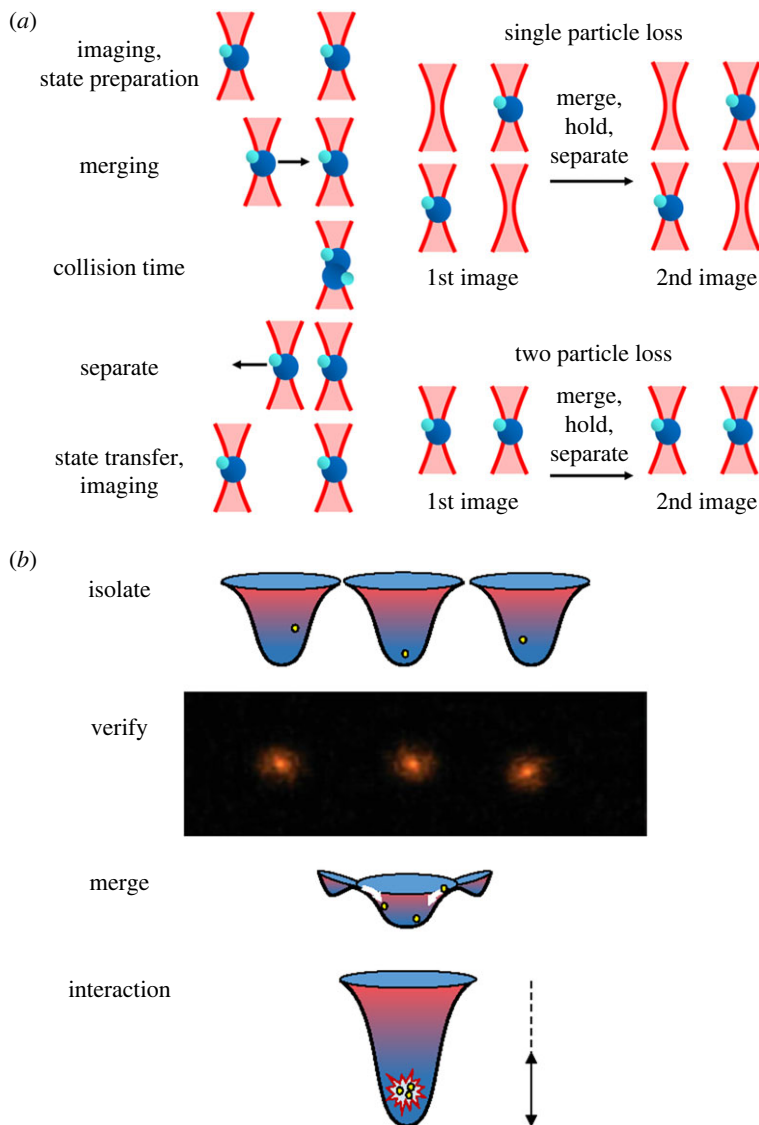
Figure 12. (*a*) The measurement procedure for studying collisions between a pair of molecules (CaF) each prepared in a given quantum state and trapped in a singly occupied optical tweezer. Adapted from [103]. (*b*) Procedure for studying simultaneous interaction of three Rb atoms trapped initially in separate individual optical tweezers. Adapted from [157].

suppressing collisional reactive losses offers opportunities to use molecules held in tweezers for quantum simulation, e.g. of condensed matter systems (see §3b).

Three-body collisions have also been observed in tweezer traps with three Rb atoms prepared in separate optical tweezers and brought together (figure 12*b*). The three-body loss process $Rb + Rb + Rb \rightarrow Rb_2 + Rb$ was observed but they concluded that there was a strongly suppressed three-body recombination loss rate compared to previous experiments with many-atom ensembles [157]. They speculated that the suppressed loss rate may indicate *the presence of anticorrelations similar to those present in the super-Tonks-Girardeau gas, a metastable phase of attractively interacting bosons in one dimension.* These experiments point to the future observation of novel chemical/physical behaviour with such control over single particles and their interactions.

(b) Quantum computation and simulating novel states of matter

(i) Qubits and qudits

As stated earlier, in comparison with laser cooling of atoms, the laser cooling and state control of molecules is a much more complex operation, but it is frequently argued that the more complex energy level structure brings significant benefits for quantum computation and simulation [159]. A review of possibilities for quantum simulators was presented in 2021 [160], and the potential applications in quantum-materials simulation, quantum chemistry, quantum devices and transport, gravity particle physics and cosmology, and non-equilibrium quantum many-body dynamics were highlighted. In considering cold molecules as one of 10 possible platforms for quantum simulators (other platforms include, e.g. ultracold atoms, trapped ions, Rydberg atom arrays, as well as solid-state systems), they argue that *the range of frequencies of transitions in molecules, from kilohertz to hundreds of terahertz, lends itself to efficient information transduction across different platforms. The study of multiscale quantum physics, while combining with their intrinsic tunable interactions, will allow high-fidelity entanglement to be reached. Stacked multilayer fermionic polar molecules can simulate the extended-Hubbard and t-J models and topological phases, while different classes of molecules can explore models difficult to access with other platforms,* e.g. *exotic XYZ magnetism, and internal states can provide a separately tunable reservoir for simulations of open quantum systems. Crucial challenges for lattice-based quantum simulators include cooling the system to the many-body ground state, obtaining more than about 10^3 to 10^4 quantum elements, and extending the classes of molecules to simulate more models. Addressability at the single molecule level is another key goal, as well as trapping and control of cold molecules in optical tweezers.*

It was also noted that the use of microwave-addressable rotational levels of the trapped molecules could facilitate robust single-qubit operations and electric dipole coupling between adjacent molecules and could provide gate operations with a predicted fidelity greater than 99.99%; nuclear spin states in the ground rotational manifold could safeguard quantum information, acting as viable storage qubits. *The combination of long-lived rotational states with strong, switchable, dipolar interactions and noninteracting storage states for long quantum memories render ultracold polar molecules a very appealing qubit platform in a realistic system.*

The long-range interactions in a dipolar molecular system bring obvious benefits in comparison to ultracold atomic gases, although these interactions also impose limitations on coherence times. Quantum computation relies on the preparation of a coherent quantum superposition of internal states. However, such coherent superpositions of states with molecules are often extremely fragile, with experimental noise and coupling to the environment leading to rapid dephasing or decoherence, resulting in an incoherent mixture of states.

In 2021, Gregory *et al.* [161] reported a strategy for eliminating problems of decoherence for ultracold molecules. Working with an optically trapped ultracold RbCs gas, they studied the coherence lifetime of superpositions of a pair of hyperfine states of the RbCs molecules. They determined the magnetic field strength for which the two hyperfine states have an identical magnetic moment. At that field, the coherence lifetime is insensitive to variations in external magnetic fields—noise that would otherwise cause decoherence. They also eliminated the differential light shift between the states (caused by the trapping light), which would also lead to decoherence, by adjusting the angle between the linearly polarized trap light and the applied magnetic field to be equal to a 'magic angle' of 55°—this resulted in a coherence time exceeding 5.6 s. They state that the methodology is compatible with the confinement of molecules in optical tweezers or three-dimensional optical lattices and could be applied to the complete range of bi-alkali molecules that are currently being studied. In parallel with those measurements, Doyle and co-workers [162] measured the rotational coherence time of CaF molecules in optical tweezer traps. A 93(7) ms coherence time for rotational state qubits was reported, and they suppressed inhomogeneous broadening due to the differential polarizability between the qubit states by tuning the tweezer polarization and applied magnetic field to a 'magic' angle. They reported that a single spin-echo pulse is able to extend the coherence time to nearly 0.5 s. These recent measurements mark a potentially very significant step forward

towards the creation of a quantum computer using ultracold molecules, as the reported coherence times are considerably longer than the predicted millisecond timescale required for qubit gate operations.

The potential to take advantage of the more complex energy level structure of molecules as 'qudit' elements in quantum simulation and computing was discussed by Sawant *et al.* [163]. Qudits are higher dimensional multi-level systems, compared to two-dimensional qubits, and have some potential advantages in terms of scalability. It is postulated that computations that would go beyond the capabilities of any current classical computer (quantum supremacy) would require about 50 qubits, but only 15 ten-level qudits. The time required to carry out gate operations using *d*-dimensional qudits could potentially be reduced by a factor of log *d*. The authors also highlight that the use of qudits leads to increased robustness and improvements for quantum error-correcting codes. Thus, molecules are attractive as potential 'qudits', and they considered polar molecules such as CaF or RbCs trapped in an optical tweezer offering single-particle addressability and detection, combined with easy scaling up to arrays of approximately 100 traps. They identified an appropriate four-level energy level system for these molecules using the rotational and hyperfine structure (originating from the nuclear magnetic moments in these molecules) and manipulation of energies with magnetic fields. Decoherence is a major potential limitation, considered in this paper, but the authors conclude that electronic states of $^1\Sigma$ symmetry (e.g. RbCs) are particularly resistant to the decoherence mechanisms considered (mainly electromagnetic noise due to the fluctuations of the trapping lasers).

The use of *molecular ions* as qubits or qudits is also an attractive possibility, given the very long trapping times that are possible with ions in deep ion traps. Zhu *et al.* [164] performed high-resolution spectroscopy on the SiO$^+$ molecular ion, and in that work have discussed the use of this molecule as a qubit. Preparing the molecule in a single hyperfine level with the second state of the qubit being an excited hyperfine level, they create a qubit that can be prepared in an arbitrary qubit state using microwave spectroscopy and observed that this is insensitive to electric and magnetic field noises even in an ion trap.

(ii) Novel condensed matter physics

One of the driving forces to develop sources of ultracold polar molecules has been to take advantage of the long-range anisotropic dipolar interactions, which, when coupled with low temperatures and optical array trapping, have the potential to generate novel phases of matter with exotic properties that are controlled by topology. For example, there have been theoretical proposals to use arrays of dipolar molecules trapped in deep optical lattices to generate disordered quantum magnets (quantum spin liquids) [165], Weyl semimetals [166] and fractional Chern insulators [167].

A more recent example of such work is the design of an experimental realization of a Hopf Insulator [156]—a topological insulator phase of condensed matter (i.e. one with conducting surface states but bulk insulator behaviour) that has been theoretically predicted but not observed in the laboratory. The realization requires long-range spin-hopping between lattice sites, and spin-orbit coupling that creates anisotropic hopping. The authors propose that this could be created/simulated using a deep three-dimensional optical lattice of polar KRb molecules, in which the molecules have an active rotational degree of freedom (within the lattice site), and the 'spin-hopping' is actually an exchange of molecular rotational excitation between sites. The lattice consists of alternating sublayers in which the molecules are oriented parallel to the two-dimensional layer and perpendicular to it in the A and B layers, respectively (controlled by different intensity levels of the excitation layer using four pairs of counter-propagating laser beams) figure 11. Applied fields (magnetic and electric) are used to tune the $J = 0$ and $J = 1$ energy levels into resonance, and then this degeneracy is lifted by the interaction of the light intensity with the polarizability. The dipolar interaction between the molecules is 'designed' in such a way as to drive $\Delta M = 1$ exchange of rotational interaction between sites, which is equivalent (in terms of the Hamiltonian) to spin-hopping induced by the spin-orbit interaction in conventional

condensed matter systems, and is a requirement for facilitating Hopf Insulator behaviour. While this lattice has not yet been fully implemented, the experimental parameters (static and AC (light) fields) are all feasible, and as discussed earlier the independent control of the quantum states of molecules in adjacent layers has been demonstrated in a stack of two-dimensional lattices [155].

(c) Precision measurement to test models of particle physics and fundamental constants

Given the low velocity of cold and ultracold molecules, and the ability to confine them in a localized region of space on a long timescale, there are significant benefits for precision spectroscopic measurement. One driving force behind ultra-high-precision spectroscopic measurement is to relate the high-precision results to aspects of fundamental physics—these include efforts to measure the electric dipole moment of the electron, the Schiff moment of the nucleus, and the time variation of fundamental constants, such as the proton to electron mass ratio. Spectroscopic measurements can potentially provide a signature of phenomena such as CP violation (violation of charge-conjugation parity symmetry), which has been an important component in some proposed cosmological explanations of the dominance of matter over antimatter in the universe, the preponderance of specific enantiomers of chiral molecules in nature, and in the study of weak interactions for particle physics.

An example of such current effort is the experiments of De Mille and co-workers who work with Thallium Fluoride TlF to measure CP violation through measuring the Schiff moment of the nucleus. The Schiff moment arises from the finite size of the nucleus [168] and is a charge displacement with an asymmetric distribution along the spin axis, equivalent to a charge density on the nuclear surface proportional to $\cos \theta$, where θ is the angle from the nuclear magnetic moment $\mathbf{I}$.

The experiment being developed effectively involves making a Thallium nuclear magnetic resonance (NMR) measurement by measuring the time-dependent phase shift of a prepared hyperfine state of the TlF molecule which is converted into a population difference on the Thallium nucleus. The Schiff moment should make a very small contribution to the transition frequency, which is nevertheless enhanced by many orders of magnitude in the molecule (relative to an isolated Tl atom) by the coupling to the molecular dipole moment and axis.

The experiment involves a sequence of generating a cryogenic buffer gas beam of TlF, rotational cooling of the molecules, hyperfine state preparation, driving the NMR transition, further quantum state manipulation and preparation and state readout using laser-induced fluorescence (LIF). A statistical sensitivity to the CP violation-induced energy of 50 nHz is anticipated, assuming 300 h measurement at a 50 Hz repetition rate. This would correspond to a roughly 2500-fold improvement over the previous best measurements of the ^{205}Tl Nuclear Schiff Moment, which it is asserted would correspond to a significantly improved sensitivity over the current best limits.

In other work, cold and ultracold molecule techniques are being used in experiments designed to measure the electron dipole moment (EDM—an asymmetry in the charge distribution of an electron)—another signature of CP violation and (if observed) a breakdown of the standard model of particle physics. To date, the EDM has been measured to be zero to within the error limits of the set up, and that implies a value $|d_e| < 9.4 \times 10^{-29}$ e cm (90% confidence) [169]. The objectives of current experiments are to reduce error bars to a level where a finite value can be measured for comparison with the breakdown of the standard model of particle physics. The current status of EDM measurements has been reviewed recently by Fitch & Tarbutt [63]. Cornell and co-workers are using spectroscopic measurements with trapped molecular ions HfF$^+$ and TlF$^+$ for this purpose [170]. In their recent work with hundreds or thousands of trapped molecular ions, the use of a resonant photodissociation spectroscopy technique is employed, which is molecular-orientation-resolved, to monitor state control and readout. The spectroscopic level shifts should be highly sensitive to the electron dipole moment in these molecules and are proposed to go beyond the current sensitivity limits made on the ThO molecule in 2018. An improvement on the
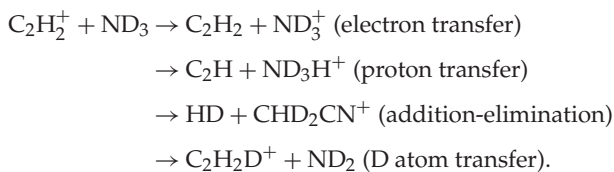
upper limit for the magnitude of dipole moment, to -4×10^{-30} e cm at 90% confidence, from the trapped molecular ion measurements, has been very recently announced [171].

Bethlem and co-workers [172] are currently establishing a 'molecular fountain' approach to enable precision spectroscopic measurements that may reveal information about the time variation of molecular constants—for example by performing very high-precision spectroscopy of ND_3 they intend to observe the time variation of the proton to electron mass ratio. The molecules are directed vertically through a Stark decelerator and reach a sufficiently low velocity such that gravity will turn them round. The long observation time will enable a very high-precision Ramsey interference measurement.

4. Outlook for the 2020s

In this article, the remarkable progress in controlling and manipulating cold and ultracold molecules in the last few years is highlighted, and this is very rapidly leading to new, exciting applications of those capabilities, and new ideas of how to exploit these techniques. These include efforts: to understand the behaviour of chemical processes at extremely low temperatures, with particular focus on 'the quantum regime' for reactions, and including the relevance in astrochemistry; to make high-precision measurements taking advantage of the small Doppler effect and long trapping times in 'almost stationary' molecules; to explore the possibility for the creation of arrays of molecular qubits and qudits; and to create or simulate novel exotic states of matter. The recent advances have been dramatic, and it is likely that such applications will continue to be developed over the remainder of this decade.

In the field of cold and ultracold chemistry, some of the interesting challenges to explore include creating a greater diversity of chemical species at such temperatures, particularly in the ultracold, and exploiting these so that reactions of true chemical complexity can be investigated. While collisional experiments with atoms and diatoms are already revealing very interesting physics, reactions involving polyatomic species bring new levels of complexity and potentially new physics. The overwhelming majority of chemical reactions do not simply produce a single pair of product species—much of the task of chemical synthesis revolves around controlling conditions so as to increase the yield and selectivity for specific products, in competition with potential side reactions. Even for a relatively simple gas-phase ion–molecule reaction such as $NH_3{}^+ + C_2H_2$ there are already four energetically available product channels even at cold temperatures:

$$C_2H_2^+ + ND_3 \rightarrow C_2H_2 + ND_3^+ \text{ (electron transfer)}$$
$$\rightarrow C_2H + ND_3H^+ \text{ (proton transfer)}$$
$$\rightarrow HD + CHD_2CN^+ \text{ (addition-elimination)}$$
$$\rightarrow C_2H_2D^+ + ND_2 \text{ (D atom transfer)}.$$

The branching ratio between the four channels is controlled by the detailed dynamics on multiple potential energy surfaces, and the ability to attain fine control of experimental parameters at cold and ultracold temperatures, such as collision energy and internal quantum states can potentially modify the branching ratios.

While the ultracold is likely to provide the ultimate medium for controlling the reactant quantum states, the additional vibrational and rotational degrees of freedom in many-atom molecules will bring new complications and challenges for both experimentalists and theorists, while the multipole moments of molecules (e.g. dipole or quadrupole) bring challenges for isolation from external forces.

Future studies using ultracold polyatomic molecules may include the intriguing possibility to create chiral ultracold species and study collisional processes of these. Given developments in laser cooling of polyatomic molecules, and in sensitive enantiomer-selective detection methods [173,174], such studies may become a reality in the next few years. The development of optical
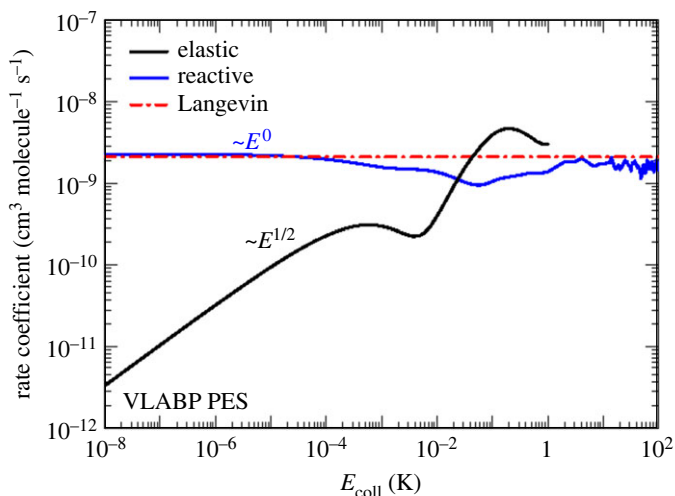
Figure 13. Quantum dynamics calculation of the rate coefficient for reactive collisions and elastic collisions over a range of 10 orders of magnitude in temperature for the $D^+ + H_2$ ($v = 0, j = 0$) reaction. The calculated rates are compared to the classical capture theory Langevin rate. Note the resonance effects observed in the reactive collisions at the higher energy range and the more monotonic (but non-Langevin) behaviour at the low-temperature end. Adapted from [175].

cycling centres, as described in §2a, may also provide opportunities ultimately for laser cooling of a wider range of more complex species.

Currently, it is difficult to draw connections between chemical behaviour in the ultracold regime and the temperatures at which many chemical reactions naturally occur (i.e. 300 K), as the kind of precision experiments that have been developed in the ultracold (e.g. using optical lattices or tweezers) could not be implemented at higher temperatures. Even drawing a link between the 'cold' and 'ultracold' regimes is hard, because most techniques do not offer the opportunity to explore the transition between these regimes. The analysis and interrogation of chemical processes tends to be set up for a particular temperature regime, as are the methods for producing the molecules. Theoretical calculations on the other hand often give results over many orders of magnitude in temperature. Figure 13 shows the calculated cross section for a simple ion–molecule reaction $D^+ + H_2$ covering over 10 orders of magnitude in temperature [175]. It remains just a dream for experimentalists to really observe the transition from the classical to the quantum regime for any chemical system as illustrated in the figure.

In the 2020s, the achievement of quantum degenerate samples of ultracold molecules has been demonstrated (see §2) at least for Fermi gases, and the possibility to achieve BEC of a dipolar gas is undoubtedly being explored in laboratories around the world. There are many intriguing questions from a chemistry perspective about how chemical reactions would occur in a coherent environment, in which every molecule is 'connected' by a common wave function to every other one, and how the condensate would evolve under such conditions—in addition to more fundamental questions about the physical properties of dipolar condensates. In an interesting recent experiment, a single Rb^+ ion was created within a BEC of Rb atoms and its diffusive motion was tracked [176]—this diffusion is likely to be an important aspect of chemistry within a BEC. The creation and tracking of single molecules in a BEC may be achievable in the future.

The observation of collisions of single molecules held in optical tweezers is a very exciting new development. In the teaching of chemistry at all levels, it has been common practice for teachers to pick up models of molecules, one in each hand and bring them together to illustrate the mechanism of a reaction. We might also draw diagrams or show computer simulation videos to illustrate mechanisms. In 2021, Cheuk et al. [103] made a major advance in picking up two actual molecules using optical tweezers and bringing them together and observing the outcome

of the collision of those molecules, described as either chemical reaction or complex formation. Undoubtedly, the possibilities to manipulate these molecules and study the impact of those quantum state manipulations on reaction—for example to control spatial orientation—will be developed, and possibly three-body (or many-body) processes will be studied directly with three (or many) molecules, each trapped in an individual tweezer, as has already been demonstrated for one three-atom system [157].

The application of ultracold molecule techniques to quantum computation and simulation remains very much in its infancy, and there will continue to be experiments that test the feasibility of establishing qubits and qudits using ultracold molecules, including understanding decoherence mechanisms and lifetimes, and the practicalities of scale up. Significant progress in eliminating decoherence mechanisms for some specific molecular systems has been recently demonstrated. The demonstration of the trapping of molecules in arrays of optical tweezers is an exciting direction to pursue in the context of controlling multiple qubits or qudits. Recent experiments have reported the complete assembly of a square array of 324 optically trapped ultracold Rb atoms each held in an individual tweezer [102] and linear tweezer arrays are already possible for molecules. It has been demonstrated that reactions or inelastic collisions can be switched on or off by microwave dressing in these highly controlled environments—and it is interesting to note that chemists tend to be more excited by the enhancement of the reactivity, while physicists developing quantum computation systems are more interested in suppressing reactivity!

There have been considerable investments in complex experiments for high-precision spectroscopic measurements for fundamental physics in recent years—although the budgets for such experiments are absolutely dwarfed by budgets for particle-physics experiments. We can expect an acceleration of progress in these measurements given the levels of quantum control that are now achievable, and these will possibly contribute to major advances in cosmology and the models of particle physics. The ability to decelerate and trap heavy molecules [115] is highly significant in this respect as in many cases these are the species which are most likely to reveal the fundamental physical properties.

Overall this is a very exciting moment for cold and ultracold molecule studies. Much of the work over the last 20–30 years is reaching a level of maturity that will start to come to fruition. Theoretical approaches have also been developed very substantially hand in hand with experiments, and undoubtedly current measurements are already pushing theoreticians to develop these further [150,151]. These experiments remain highly complex and, in some cases, stretch technical capabilities to their current limits; but the opportunity is now there to grasp these developments and really demonstrate the exciting science that is possible.

References

1. Heazlewood BR, Softley TP. 2015 Low-temperature kinetics and dynamics with Coulomb crystals. *Ann. Rev. Phys. Chem.* **66**, 475. (doi:10.1146/annurev-physchem-040214-121527)
2. Smith IWM. 2006 Reactions at very low temperatures: gas kinetics at a new frontier. *Angew. Chem. Int. Ed.* **45** 2842–2861. (doi:10.1002/anie.200502747)
3. Sahai R, Vlemmings WHT, Nyman LA. 2017 The coldest place in the universe: probing the ultra-cold outflow and dusty disk in the Boomerang. *Ap. J.* **841**, 110 (16pp). (doi:10.3847/1538-4357/aa6d86)
4. Metcalf HJ, Straten P. 1999 *Laser cooling and trapping, graduate texts in contemporary physics*. Berlin, Germany: Springer.
5. Bell MT, Softley TP. 2009 Ultracold molecules and ultracold chemistry. *Mol. Phys.* **107**, 99–132. (doi:10.1080/00268970902724955)

6. McClelland BJJ, Steele AV, Knuffman B, Twedt KA, Schwarzkopf A, Wilson TM. 2016 Bright focused ion beam sources based on laser-cooled atoms. *Appl. Phys. Rev.* **3**, 011302. (doi:10.1063/1.4944491)

7. Tarbutt MR. 2019 Laser cooling of molecules. *Contemp. Phys.* **59**, 356–376. (doi:10.1080/00107514.2018.1576338)

8. Valtolina G, Matsuda K, Tobias WG, Li J-R, De Marco L, Ye J. 2020 Dipolar evaporation of reactive molecules to below the Fermi temperature. *Nature* **588**, 239. (doi:10.1038/s41586-020-2980-7)

9. Stuhl BK, Hummon MT, Yeo M, Quéméner G, Bohn JL, Ye J. 2012 Evaporative cooling of the dipolar hydroxyl radical. *Nature* **492**, 396–400. (doi:10.1038/nature11718)

10. van de Meerakker SYT, Bethlem HL, Vanhaecke N, Meijer G. 2012 Manipulation and control of molecular beams. *Chem. Rev.* **112**, 4828–4878. (doi:10.1021/cr200349r)

11. Meijer G. 2021 Manipulation and control of molecular beams: the development of the Stark-decelerator. In *Molecular beams in physics and chemistry: from Otto Stern's pioneering exploits to present-day feats chapter 20* (eds B Friedrich, H Schmidt-Böcking), p. 463. Cham: Springer Nature Switzerland. https://doi.org/10.1007/978-3-030-63963-1.

12. Hogan SD, Motsch M, Merkt F. 2011 Deceleration of supersonic beams using inhomogeneous electric and magnetic fields. *Phys. Chem. Chem. Phys.* **13**, 18705–18723. (doi:10.1039/c1cp21733j)

13. Narevicius E, Raizen MG. 2012 Toward cold chemistry with magnetically decelerated supersonic beams. *Chem. Rev.* **112**, 4879–4889. (doi:10.1021/cr2004597)

14. Procter SR, Yamakita Y, Merkt F, Softley TP. 2003 Controlling the motion of hydrogen molecules. *Chem. Phys. Lett.* **374**, 667. (doi:10.1016/S0009-2614(03)00812-1)

15. Hogan SD. 2016 Rydberg-Stark deceleration of atoms and molecules. *EPJ Tech. Instrum.* **3**, 2. (doi:10.1140/epjti/s40485–015–0028–4)

16. Rangwala SA, Junglen T, Rieger T, Pinkse PWH, Rempe G. 2003 Continuous source of translationally cold dipolar molecules. *Phys. Rev. A* **67**, 043406. (doi:10.1103/PhysRevA.67.043406)

17. Twyman KS, Bell MT, Heazlewood BR, Softley TP. 2014 Production of cold beams of ND_3 with variable rotational state distributions by electrostatic extraction of He and Ne buffer gas cooled beams J. *Chem. Phys.* **141**, 024308. (doi:10.1063/1.4885855)

18. Hutzler NR, Lu H-I, Doyle JM. 2012 The buffer gas beam: an intense, cold, and slow source for atoms and molecules. *Chem. Rev.* **112**, 4803–4827. (doi:10.1021/cr200362u)

19. Steer EW, Petralia LS, Western CM, Heazlewood BR, Softley TP. 2016 Measurement of the orientation of buffer-gas-cooled, electrostatically-guided ammonia molecules. *J. Mol. Spectrosc.* **332**, 94. (doi:10.1016/j.jms.2016.11.003)

20. Toscano J, Rennick CJ, Softley TP, Heazlewood BR. 2018 A magnetic guide to purify radical beams. *J. Chem. Phys.* **149**, 174201. (doi:10.1063/1.5053656)

21. deCarvalho R, Doyle JM, Friedrich B, Guillet T, Kim J, Patterson D, Weinstein JD. 1999 Buffer-gas loaded magnetic traps for atoms and molecules: a primer. *Eur. Phys. J. D* **7**, 289–309. (doi:10.1007/s100530050572)

22. Elioff MS, Valentini JJ, Chandler DW. 2003 Subkelvin cooling NO molecules via 'Billiard-like' collisions with argon. *Science* **302**, 1940–1943. (doi:10.1126/science.1090679)

23. Strebel M, Stienkemeier F, Mudrich M. 2010 Improved setup for producing slow beams of cold molecules using a rotating nozzle. *Phys. Rev. A* **81**, 033409. (doi:10.1103/PhysRevA.81.033409)

24. Gupta M, Herschbach D. 2001 Slowing and speeding molecular beams by means of a rapidly rotating source. *J. Phys. Chem. A* **105**, 1626–1637. (doi:10.1021/jp002640u)

25. Chervenkov S, Wu X, Bayerl J, Rohlfes A, Gantner T, Zeppenfeld M, Rempe G. 2014 Continuous centrifuge decelerator for polar molecules. *Phys. Rev. Lett.* **112**, 013001. (doi:10.1103/PhysRevLett.112.013001)

26. Son H, Park JJ, Ketterle W, Jamison AO. 2020 Collisional cooling of ultracold molecules. *Nature* **580**, 197. (doi:10.1038/s41586-020-2141-z)

27. Hudson EJ. 2016 Sympathetic cooling of molecular ions with ultracold atoms Hudson. *EPJ Techn. Instrum.* **3**, 8. (doi:10.1140/epjti/s40485-016-0035-0)

28. Zeppenfeld M, Englert BGU, Glöckner R, Prehn A, Mielenz M, Sommer C, van Buuren LD, Motsch M, Rempe G. 2012 Sisyphus cooling of electrically trapped polyatomic molecules. *Nature* **491**, 570–573. (doi:10.1038/nature11595)

29. Jones KM, Tiesinga E, Lett PD, Julienne PS. 2006 Ultracold photoassociation spectroscopy: long-range molecules and atomic scattering. *Rev. Mod. Phys.* **78**, 483–535. (doi:10.1103/RevModPhys.78.483)

30. Ulmanis J, Repp M, Wester R, Weidemüller M. 2012 Ultracold molecules formed by photoassociation: heteronuclear dimers, inelastic collisions, and interactions with ultrashort laser pulses. *Chem. Rev.* **112**, 4890–4927. (doi:10.1021/cr300215h)

31. Danzl JG, Haller E, Gustavsson M, Mark MJ, Hart R, Bouloufa N, Dulieu O, Ritsch H, Nägerl H-C. 2008 Quantum gas of deeply bound ground state molecules. *Science* **321**, 1062–1066. (doi:10.1126/science.1159909)

32. Ni K-K *et al.* 2008 A high phase-space-density gas of polar molecules. *Science* **322**, 231–235. (doi:10.1126/science.1163861)

33. Chin C, Grimm R, Julienne P, Tiesinga E. 2010 Feshbach resonances in ultracold gases. *Rev. Mod. Phys.* **82**, 1225–1286. (doi:10.1103/RevModPhys.82.1225)

34. Park JW, Will SA, Zwierlein MW. 2015 Ultracold dipolar gas of fermionic $^{23}Na^{40}K$ molecules in their absolute ground state. *Phys. Rev. Lett.* **114**, 205302. (doi:10.1103/PhysRevLett.114.205302)

35. Weckesser P, Thielemann F, Wiater D, Wojciechowska A, Karpa L, Jachymski K, Tomza M, Walker T, Schaetz T. 2021 Observation of Feshbach resonances between a single ion and ultracold atoms. *Nature* **600**, 429. (doi:10.1038/s41586-021-04112-y)

36. Eardley JS, Warner N, Deng LZ, Carty D, Wrede E. 2017 Magnetic trapping of SH radicals. *Phys. Chem. Chem. Phys.* **19**, 8423–8427. (doi:10.1039/C7CP00458C)

37. Rennick C, Lam J, Doherty W, Softley TP. 2014 Magnetic trapping of cold bromine atoms . *Phys. Rev. Lett.* **112**, 023002. (doi:10.1103/PhysRevLett.112.023002)

38. Henson AB, Gersten S, Shagam Y, Narevicius J, Narevicius E. 2012 Observation of resonances in Penning ionization reactions at sub-Kelvin temperatures in merged beams. *Science* **338**, 234. (doi:10.1126/science.1229141)

39. Allmendinger P, Deiglmayr J, Schullian O, Höveler K, Agner JA, Schmutz H, Merkt F. 2016 New method to study ion–molecule reactions at low temperatures and application to the $H_2^++H_2\rightarrow H_3^++H$ reaction. *Chem. Phys. Chem.* **17**, 3596–3608. (doi:10.1002/cphc.201600828)

40. Gawlas K, Hogan SD. 2020 Rydberg-state-resolved resonant energy transfer in cold electric-field controlled intrabeam collisions of NH_3 with Rydberg He atoms. *J. Phys. Chem. Lett.* **11**, 83–87. (doi:10.1021/acs.jpclett.9b03290)

41. Perreault WE, Mukherjee N, Zare RN. 2019 HD (v = 1, j = 2, m) orientation controls HD–He rotationally inelastic scattering near 1 K. *J. Chem. Phys.* **150**, 174301. (doi:10.1063/1.5096531)

42. Mackenzie SR, Softley TP. 1994 New experimental method for studying rotationally state-selected ion-molecule reactions. *J. Chem. Phys.* **101**, 10609. (doi:10.1063/1.467875)

43. Foot CJ. 2005 *Atomic Physics*. New York: Oxford University Press.

44. Vilas NB, Hallas C, Anderegg L, Robichaud P, Winnicki A, Mitra D, Doyle JM. 2022 Magneto-optical trapping and sub-Doppler cooling of a polyatomic molecule. *Nature* **606**, 70–74. (doi:10.1038/s41586-022-04620-5)

45. Williams HJ, Truppe JS, Hambach M, Caldwell L, Fitch NJ, Hinds EA, Sauer BE, Tarbutt MR. 2017 Characteristics of a magneto-optical trap of molecules. *New J. Phys.* **19**, 113035. (doi:10.1088/1367-2630/aa8e52)

46. Jurgilas S, Chakraborty A, Rich CJH, Sauer BE, Frye MD, Hutson JM, Tarbutt MR. 2020 Collisions in a dual-species magneto-optical trap of molecules and atoms. *New J. Phys.* **23**, 075004. (doi:10.1088/1367-2630/ac0c9a)

47. Bethlem HL, Berden G, Crompvoets FMH, Jongma RT, van Roij AJA, Meijer G. 2000 Electrostatic trapping of ammonia molecules. *Nature* **406**, 491–494. (doi:10.1038/35020030)

48. Fitch NJ, Parazzoli LP, Lewandowski HJ. 2020 Collisions between ultracold atoms and cold molecules in a dual electrostatic-magnetic trap. *Phys. Rev. A* **101**, 032703. (doi:10.1103/PhysRevA.101.032703)

49. Kaufman AM, Ni K-K. 2021 Quantum science with optical tweezer arrays of ultracold atoms and molecules. *Nat. Phys.* **17**, 1324–1333. (doi:10.1038/s41567-021-01357-2)

50. Moses SA, Covey JP, Miecnikowski MT, Yan B, Gadway B, Ye J, Jin DS. 2015 Creation of a low-entropy quantum gas of polar molecules in an optical lattice. *Science* **350**, 659. (doi:10.1126/science.aac6400)

51. Liu Y, Vashishta M, Djuricanin P, Zhou S, Zhong W, Mittertreiner T, Carty D, Momose T. 2017 Magnetic trapping of cold methyl radicals. *Phys. Rev. Lett.* **118**, 093201. (doi:10.1103/PhysRevLett.118.093201)

52. Riedel J, Hoekstra S, Jäger W, Gilijamse JJ, van de Meerakker SYT, Meijer G. 2011 Accumulation of stark-decelerated NH molecules in a magnetic trap. *Eur. Phys. J. D* **65**, 161–166. (doi:10.1140/epjd/e2011-20082-7)

53. Caldwell L, Williams HJ, Fitch NJ, Aldegunde J, Hutson JM, Sauer BE, Tarbutt MR. 2020 Long rotational coherence times of molecules in a magnetic trap. *Phys. Rev. Lett.* **124**, 063001. (doi:10.1103/PhysRevLett.124.063001)

54. Hummon MT, Tscherbul TV, Kłos J, Lu H-I, Tsikata E, Campbell WC, Dalgarno A, Doyle JM. 2011 Cold N + NH collisions in a magnetic trap. *Phys. Rev. Lett.* **106**, 053201. (doi:10.1103/PhysRevLett.106.053201)

55. Wester R. 2009 Radiofrequency multipole traps: tools for spectroscopy and dynamics of cold molecular ions. *J. Phys. B* **42**, 154001. (doi:10.1088/0953-4075/42/15/154001)

56. Asvany O, Brünken S, Kluge L, Schlemmer S. 2014 COLTRAP: a 22-pole ion trapping machine for spectroscopy at 4 K. *Appl. Phys. B* **114**, 203–211. (doi:10.1007/s00340-013-5684-y)

57. Gerlich D. 1995 Ion-neutral collisions in a 22-pole trap at very low energies. *Phys. Scr.* **1995**, 256. (doi:10.1088/0031-8949/1995/T59/035)

58. Julienne PS. 2018 Quo vadis now, cold molecules. *Nat. Phys.* **14**, 873–880. (doi:10.1038/s41567-018-0260-3)

59. Georgescu I. 2020 25 years of BEC. *Nat. Rev. Phys.* **2**, 396. (doi:10.1038/s42254–020–0211–7)

60. Heazlewood BR, Softley TP. 2021 Towards chemistry at absolute zero. *Nat. Rev. Chem.* **5**, 125. (doi:10.1038/s41570-020-00239-0)

61. Bohn JL, Rey AM, Ye J. 2017 Cold molecules: progress in quantum engineering of chemistry and quantum matter. *Science* **357**, 1002–1010. (doi:10.1126/science.aam6299)

62. Balakrishnan N. 2016 Perspective: ultracold molecules and the dawn of cold controlled chemistry. *J. Chem. Phys.* **145**, 150901. (doi:10.1063/1.4964096)

63. Fitch NJ, Tarbutt MR. 2021 From hot beams to trapped ultracold molecules: motivations, methods and future directions. In *Molecular beams in physics and chemistry: from Otto Stern's pioneering exploits to present-day feats* (eds B Friedrich, H Schmidt-Böcking), p. 49. Cham, Switzerland: Springer.

64. Dulieu O, Osterwalder A (eds). 2018 *Cold chemistry: molecular scattering and reactivity near absolute zero*. Cambridge, UK: Royal Society of Chemistry.

65. Wall TE. 2016 Preparation of cold molecules for high-precision measurements. *J. Phys. B: At. Mol. Opt. Phys.* **49**, 243001. (doi:10.1088/0953-4075/49/24/243001)

66. Toscano J, Lewandowski H, Heazlewood BR. 2020 Cold and controlled chemical reaction dynamics. *Phys. Chem. Chem. Phys.* **22**, 9180–9194. (doi:10.1039/D0CP00931H)

67. Liu Y, Ni K-K. 2022 Bimolecular chemistry in the ultracold regime. *Annu. Rev. Phys. Chem.* **73**, 73–96. (doi:10.1146/annurev-physchem-090419-043244)

68. Zhang D, Willitsch S. 2018 Cold chemistry: molecular scattering and reactivity near absolute zero, chapter 10. In *Cold chemistry: molecular scattering and reactivity near absolute zero* (eds O Dulieu, A Osterwalder). Cambridge, UK: Royal Society of Chemistry.

69. Jansen P, Merkt F. 2020 Manipulating beams of paramagnetic atoms and molecules using inhomogeneous magnetic fields. *Prog. Nucl. Magn. Reson. Spectrosc.* **120–121**, 118–148. (doi:10.1016/j.pnmrs.2020.08.002)

70. Heazlewood BR. 2021 Quantum-state control and manipulation of paramagnetic molecules with magnetic fields. *Annu. Rev. Phys. Chem.* **72**, 353–373. (doi:10.1146/annurev-physchem-090419–053842)

71. Friedrich B, Schmidt-Böcking H (eds). 2021 *Molecular beams in physics and chemistry: from Otto Stern's pioneering exploits to present-day feats*. Berlin, Germany: Springer.

72. Truppe S, Williams HJ, Hambach M, Caldwell L, Fitch NJ, Hinds EA, Sauer BE, Tarbutt MR. 2017 Molecules cooled below the Doppler limit. *Nat. Phys.* **13**, 1173–1176. (doi:10.1038/nphys4241)

73. Barry JF, McCarron DJ, Norrgard EB, Steinecker MH, DeMille D. 2014 Magneto-optical trapping of a diatomic molecule. *Nature* **512**, 286–289. (doi:10.1038/nature13634)

74. Ding S, Wu Y, Finneran IA, Burau JJ, Ye J. 2020 Sub-Doppler cooling and compressed trapping of YO molecules at μK temperatures. *Phys. Rev. X* **10**, 021049. (doi:10.1103/PhysRevX.10.021049)

75. McNally RL, Kozyryev I, Vazquez-Carson S, Wenz K, Wang T, Zelevinsky T. 2020 Optical cycling, radiative deflection and laser cooling of barium monohydride (^{138}Ba^{1}H). *New J. Phys.* **22**, 083047. (doi:10.1088/1367-2630/aba3e9)

76. Yan K, Wei B, Yin Y, Xu S, Xu L, Xia M, Gu R, Xia Y, Yin J. 2020 A new route for laser cooling and trapping of cold molecules: intensity-gradient cooling of MgF molecules using localized hollow beams. *New J. Phys.* **22**, 033003. (doi:10.1088/1367-2630/ab7253)

77. Kogel K, Rockenhäuser M, Albrecht R, Langen T. 2021 A laser cooling scheme for precision measurements using fermionic barium monofluoride (^{137}Ba^{19}F) molecules. *New J. Phys.* **23**, 095003. (doi:10.1088/1367-2630/ac1df2)

78. Walter N, Seifert J, Truppe S, Schewe HC, Sartakov BG, Meijer G. 2022 Spectroscopic characterization of singlet–triplet doorway states of aluminium monofluoride. *J. Chem. Phys.* **156**, 184301. (doi:10.1063/5.0088288)

79. Lim JJ, Almond JR, Trigatzis MA, Devlin JA, Fitch NJ, Sauer BE, Tarbutt MR, Hinds EA. 2018 Laser cooled YbF molecules for measuring the electron's electric dipole moment. *Phys. Rev. Lett.* **120**, 123201. (doi:10.1103/PhysRevLett.120.123201)

80. Schnaubelt JC, Shaw JC, McCarron DJ. 2021 Cold CH radicals for laser cooling and trapping. (http://arxiv.org/abs/2109.03953) [physics.atom-ph].

81. Kozyryev I, Baum L, Matsuda K, Augenbraun BL, Anderegg L, Sedlack AP, Doyle JM. 2017 Sisyphus laser cooling of a polyatomic molecule. *Phys. Rev. Lett.* **118**, 173201. (doi:10.1103/PhysRevLett.118.173201)

82. Sawaoka H, Frenett A, Nasir A, Ono T, Augenbraun BL, Steimle TC, Doyle JM. 2022 Zeeman-sisyphus deceleration for heavy molecules with perturbed excited-state structure. (http://arxiv.org/abs/2210.10859v1)

83. Mitra D, Vilas NB, Hallas C, Anderegg L, Augenbraun BL, Baum L, Miller C, Raval H, Doyle JM. 2020 Direct laser cooling of a symmetric top molecule. *Science* **369**, 1366–1369. (doi:10.1126/science.abc5357)

84. Yang Q-S, Song C, Huang J, Fang M, Wan M, Yang Y. 2022 The feasibility of laser cooling: an ab initio investigation of ^{88}Sr^{35}Cl including the hyperfine structure. *Mol. Phys.* **120**, e2145244. (doi:10.1080/00268976.2022.2145244)

85. Augenbraun BL, Frenett A, Sawaoka H, Hallas C, Vilas NB, Nasir A, Lasner ZD, Doyle JM. 2021 Zeeman-sisyphus deceleration of molecular beams. *Phys. Rev. Lett.* **127**, 263002. (doi:10.1103/PhysRevLett.127.263002)

86. Dickerson CE, Guo H, Shin AJ, Augenbraun BL, Caram JR, Campbell WC, Alexandrova AN. 2021 Franck-Condon tuning of optical cycling centers by organic functionalization. *Phys. Rev. Lett.* **126**, 123002. (doi:10.1103/PhysRevLett.126.123002)

87. Mitra D *et al.* 2022 Pathway towards optical cycling and laser cooling of functionalized arenes. ((http://arxiv.org/abs/2202.01685v3).

88. Yan ZZ, Park JW, Ni Y, Loh H, Will S, Karman T, Zwierlein M. 2020 Resonant dipolar collisions of ultracold molecules induced by microwave dressing. *Phys. Rev. Lett.* **125**, 063401. (doi:10.1103/PhysRevLett.125.063401)

89. Schindewolf A, Bause R, Chen X-Y, Duda M, Karman T, Bloch I, Luo X-Y. 2022 Evaporation of microwave-shielded polar molecules to quantum degeneracy. *Nature* **607**, 677. (doi:10.1038/s41586-022-04900-0)

90. Wu X, Gantner T, Zeppenfeld M, Chervenkov S, Rempe G. 2016 Thermometry of guided molecular beams from a cryogenic buffer-gas cell. *Chemphyschem* **17**, 3631–3640. (doi:10.1002/cphc.201600559)

91. Mohammadi A, Krükow A, Mahdian A, Deiß M, Pérez-Ríos J, da Silva Jr H, Raoult M, Dulieu O, Hecker-Denschlag J. 2021 Life and death of a cold BaRb$^+$ molecule inside an ultracold cloud of Rb atoms. *Phys. Rev. Res.* **3**, 013196. (doi:10.1103/PhysRevResearch.3.013196)

92. Miossec C, Hejduk M, Pandey R, Coughlan NJA, Heazlewood BR. 2022 Design and characterization of a cryogenic linear Paul ion trap for ion–neutral reaction studies. *Rev. Sci. Instrum.* **93**, 033201. (doi:10.1063/5.0080458)

93. Viteau M, Chotia A, Allegrini M, Bouloufa N, Dulieu O, Comparat D, Pillet P. 2008 Optical pumping and vibrational cooling of molecules. *Science* **321**, 232–234. (doi:10.1126/science.1159496)

94. Cournol A, Pillet P, Lignier H, Comparat D. 2017 Rovibrational optical cooling of a molecular beam. *Phys. Rev. A* **97**, 031401. (doi:10.1103/PhysRevA.97.031401)

95. Wang X-Y *et al.* 2021 Magnetic Feshbach resonances in collisions of ^{23}Na^{40}K with ^{40}K. *New J. Phys.* **23**, 115010. (doi:10.1088/1367-2630/ac3318)

96. Su Z, Yang H, Cao J, Wang X-Y, Rui J, Zhao B, Pan J-W. 2022 Resonant control of elastic collisions between ^{23}Na^{40}K molecules and ^{40}K atoms. *Phys. Rev. Lett.* **129**, 033401. (doi:10.1103/PhysRevLett.129.033401)

97. Yang H, Wang X-Y, Su Z, Cao J, Zhang D-C, Rui J, Zhao B, Bai C-L, Pan J-W. 2022 Evidence for the association of triatomic molecules in ultracold ^{23}Na^{40}K $+$ ^{40}K mixtures. *Nature* **602**, 229. (doi:10.1038/s41586-021-04297-2)

98. Yang H, Cao J, Su Z, Rui J, Zhao B, Pan J-W. 2022 Creation of an ultracold gas of triatomic molecules from an atom–diatomic molecule mixture. *Science* **378**, 1009–1013. (doi:10.1126/science.ade6307)

99. Son H, Park JJ, Lu Y-K, Jamison AO, Karman T, Ketterle W. 2022 Control of reactive collisions by quantum interference. *Science* **375**, 1006. (doi:10.1126/science.abl7257)

100. Bird RC, Tarbutt MR, Hutson JM. 2023 Tunable Feshbach resonances in collisions of ultracold molecules in $^2\Sigma$ states with alkali-metal atoms. (http://arxiv.org/abs/2302.14687v1)

101. Holland CM, Lu Y, Cheuk LW. 2022 Bichromatic imaging of single molecules in an optical Tweezer array. (http://arxiv.org/abs/2208.12159v1)

102. Schymik K-N, Ximenez B, Bloch E, Dreon D, Signoles A, Nogrette F, Barredo D, Browaeys A, Lahaye T. 2022 In situ equalization of single-atom loading in large-scale optical tweezer arrays. *Phys. Rev. A* **106**, 022611. (doi:10.1103/PhysRevA.106.022611)

103. Cheuk LW, Anderegg L, Bao Y, Burchesky S, Yu SS, Ketterle W, Ni K-K, Doyle JM. 2020 Observation of collisions between two ultracold ground-state CaF molecules. *Phys. Rev. Lett.* **125**, 043401. (doi:10.1103/PhysRevLett.125.043401)

104. Cairncross WB, Zhang JT, Picard LRB, Yu Y, Wang K, Ni K-K. 2021 Assembly of a rovibrational ground state molecule in an optical tweezer. *Phys. Rev. Lett.* **126**, 123402. (doi:10.1103/PhysRevLett.126.123402)

105. Yichao Y *et al.* 2021 Coherent optical creation of a single molecule. *Phys. Rev. X* **11**, 031061. (doi:10.1103/PhysRevX.11.031061)

106. Højbjerre K, Hansen AK, Skyt PS, Staanum PF, Drewsen M. 2009 Rotational state resolved photodissociation spectroscopy of translationally and vibrationally cold MgH$^+$ ions: toward rotational cooling of molecular ions. *New J. Phys.* **11**, 055026. (doi:10.1088/1367-2630/11/5/055026)

107. Sinhal M, Meir Z, Najafian K, Hegi G, Willitsch S. 2020 Quantum-non-demolition state detection and spectroscopy of single trapped molecules. *Science* **367**, 1213–1218. (doi:10.1126/science.aaz9837)

108. Drewsen M. 2020 High resolution direct optical frequency comb Raman spectroscopy of single ions: from atomic fine structures to rotational spectra of molecular ions. In *Proc. SPIE 11296, Optical, Opto-Atomic and Entanglement-Enhanced Precision Metrology II, San Francisco, CA, 1–6 February 2020*, p. 19. Bellingham, WA: SPIE. (doi: 10.1117/12.2570051)

109. Patsch S, Zeppenfeld M, Koch CP. 2022 Rydberg atom-enabled spectroscopy of polar molecules via Förster resonance energy transfer. *J. Phys. Chem. Lett.* **13**, 10 728–10 733. (doi:10.1021/acs.jpclett.2c02521)

110. Guttridge A, Ruttley DK, González-Férez R, Sadeghpour HR, Adams CS, Cornish SL. 2023 Observation of Rydberg blockade due to the charge-dipole interaction between an atom and a polar molecule. (http://arxiv.org/abs/2303.06126v1)

111. Jamadagni A, Ospelkaus S, Santos L, Weimer H. 2021 Quantum Zeno-based detection and state engineering of ultracold polar molecules. *Phys. Rev. Res.* **3**, 033208. (doi:10.1103/PhysRevResearch.3.033208)

112. Karpov M, Pitzer M, Segev Y, Narevicius J, Narevicius E. 2021 Low-energy collisions between carbon atoms and oxygen molecules in a magnetic trap. *New J. Phys.* **22**, 103055. (doi:10.1088/1367-2630/abc391)

113. Tsikritea A, Diprose JA, Softley TP, Heazlewood BR. 2022 Capture theory models: an overview of their development, experimental verification, and applications to ion-molecule reactions. *J. Chem. Phys.* **57**, 060901. (doi:10.1063/5.0098552)

114. The NL-eEDM collaboration. 2018 Measuring the electric dipole moment of the electron in BaF. *Euro. Phys. J. D* **72**, 197. (doi:10.1140/epjd/e2018-90192-9)

115. Aggarwal P *et al.* 2021 Deceleration and trapping of SrF molecules. *Phys. Rev. Lett.* **127**, 173201. (doi:10.1103/PhysRevLett.127.173201)

116. Deller A, Rayment MH, Hogan SD. 2020 Slow decay processes of electrostatically trapped Rydberg NO molecules. *Phys. Rev. Lett.* **125**, 073201. (doi:10.1103/PhysRevLett.125.073201)

117. Tommey JDR, Hogan SD. 2021 Matter-wave interferometry with helium atoms in low-*l* Rydberg states. *Phys. Rev. A* **104**, 033305. (doi:10.1103/PhysRevA.104.033305)

118. Mohamed O, Wu LY, Tsikritea A, Heazlewood BR. 2021 Optimizing the intensity and purity of a Zeeman-decelerated beam. *Rev. Sci. Instrum.* **92**, 093201. (doi:10.1063/5.0061379)

119. Cremers T, Janssen N, Sweers E, van de Meerakker SYT. 2019 Design and construction of a multistage Zeeman decelerator for crossed molecular beams scattering experiments. *Rev. Sci. Instrum.* **90**, 013104. (doi:10.1063/1.5066062)

120. Plomp V, Wang X-D, Lique F, Kłos J, Onvlee J, van de Meerakker SYT. 2021 High-resolution imaging of C + He collisions using Zeeman deceleration and vacuum-ultraviolet detection. *J. Phys. Chem. Lett.* **12**, 12 210–12 217. (doi:10.1021/acs.jpclett.1c03643)

121. Damjanović T, Willitsch S, Vanhaecke N, Haak H, Meijer G, Cromiéres JP, Zhang D. 2021 A new design for a traveling-wave Zeeman decelerator: II. Experiment. *New J. Phys.* **23**, 105007. (doi:10.1088/1367-2630/ac2c2b)

122. Jankunas J, Bertsche B, Krzysztof J, Hapka M, Osterwalder A. 2014 Dynamics of gas phase Ne*+ NH$_3$ and Ne* + ND$_3$ Penning ionisation at low temperatures. *J. Chem. Phys.* **140**, 244302. (doi:10.1063/1.4883517)

123. Berteloite C *et al.* 2010 Kinetics and dynamics of the S(^{1}D$_2$) + H$_2$ → SH + H reaction at very low temperatures and collision energies. *Phys. Rev. Lett.* **105**, 203201. (doi:10.1103/PhysRevLett.105.203201)

124. Margulis B, Narevicius J, Narevicius E. 2020 Direct observation of a Feshbach resonance by coincidence detection of ions and electrons in Penning ionization collisions. *Nat. Commun.* **11**, 3553. (doi:10.1038/s41467-020-17393-0)

125. Paliwal P, Deb N, Reich DM, van der Avoird A, Koch CP, Narevicius E. 2021 Determining the nature of quantum resonances by probing elastic and reactive scattering in cold collisions. *Nat. Chem.* **94**, 94–98. (doi:10.1038/s41557-020-00578-x)

126. Tanteri S, Gordon SDS, Zou J, Osterwalder A. 2021 Study of He*/Ne*+Ar, Kr, N$_2$, H$_2$, D$_2$ chemi-ionization reactions by electron velocity-map imaging. *J. Phys. Chem.* **125**, 10 021–10 034. (doi:10.1021/acs.jpca.1c07232)

127. Höveler K, Deiglmayr J, Merkt F. 2021 Deviation of the rate of the H$_2^+$ + D$_2$ reaction from Langevin behaviour below 1 K, branching ratios for the HD$_2^+$ + H and H$_2$D$^+$ + D and product channels, and product-kinetic-energy distributions. *Mol. Phys.* **119**, e1954708. (doi:10.1080/00268976.2021.1954708)

128. Martins FBV, Zhelyazkova V, Seiler C, Merkt F. 2021 Cold ion chemistry within a Rydberg-electron orbit: test of the spectator role of the Rydberg electron in the He(n) + CO → C(n′) + O + He reaction. *New J. Phys.* **23**, 095011. (doi:10.1088/1367-2630/ac231d)

129. Höveler K, Deiglmayr J, Agner JA, Schmutz H, Merkt F. 2021 The H$_2^+$ + HD reaction at low collision energies: H$_3^+$/H$_2$D$^+$ branching ratio and product-kinetic energy distributions. *Phys. Chem. Chem. Phys.* **23**, 2676–2685. (doi:10.1039/D0CP06107G)

130. Höveler K, Deiglmayr J, Agner JA, Hahn R, Zhelyazkova V, Merkt F 2022 Observation of quantum capture in an ion-molecule reaction. *Phys. Rev. A* **106**, 052806. (doi:10.1103/PhysRevA.106.052806)

131. Zhelyazkova V, Martins FBV, Žeško M, Merkt F. 2022 Multipole-moment effects in ion–molecule reactions at low temperatures: part II – charge–quadrupole-interaction-induced suppression of the He$^+$ + N$_2$ reaction at collision energies below k$_B$·10 K. *Phys. Chem. Chem. Phys.* **24**, 2843–2858. (doi:10.1039/D1CP04798A)

132. Zhelyazkova V, Martins FBV, Merkt F. 2022 Multipole-moment effects in ion–molecule reactions at low temperatures: part III – the He$^+$ + CH$_4$ and He$^+$ + CD$_4$ reactions at low collision energies and the effect of the charge-octupole interaction. *Phys. Chem. Chem. Phys.* **24**, 16360. (doi:10.1039/D1CP05861D)

133. Zhelyazkova V, Martins FBV, Agner JA, Schmutz H, Merkt F. 2021 Multipole-moment effects in ion–molecule reactions at low temperatures: part I – ion-dipole enhancement of the rate coefficients of the He$^+$ + NH$_3$ and He$^+$ + ND$_3$ reactions at collisional energies E$_{coll}$/k$_B$ near 0 K. *Phys. Chem. Chem. Phys.* **23**, 21 606–21 622. (doi:10.1039/D1CP03116C)

134. Zhelyazkova V, Martins FBV, Agner JA, Schmutz H, Merkt F. 2020 Ion-molecule reactions below 1 K: strong enhancement of the reaction rate of the ion-dipole reaction He$^+$ + CH$_3$F. *Phys. Rev. Lett.* **125**, 263401. (doi:10.1103/PhysRevLett.125.263401)

135. de Jongh T, Besemer M, Shuai Q, Karman T, van der Avoird A, Groenenboom GC, Sebastiaan van de Meerakker YT. 2020 Imaging the onset of the resonance regime in low-energy NO-He collisions. *Science* **368**, 626–630. (doi:10.1126/science.aba3990)

136. Shuai Q, de Jongh T, Besemer M, van der Avoird A, Groenenboom G, van de Meerakker SYT. 2020 Experimental and theoretical investigation of resonances in low-energy NO–H$_2$ collisions. *J. Chem. Phys.* **153**, 244302. (doi:10.1063/5.0033488)

137. Koller M, Jung F, Phrompao J, Zeppenfeld M, Rabey IM, Rempe G. 2022 Electric-field-controlled cold dipolar collisions between trapped CH_3F molecules. *Phys. Rev. Lett.* **128**, 203401. (doi:10.1103/PhysRevLett.128.203401)

138. Kilaj A, Wang J, Straňák P, Schwilk M, Rivero U, Xu L, von Lilienfeld OA, Küpper J, Willitsch S. 2021 Conformer-specific polar cycloaddition of dibromobutadiene with trapped propene ions. *Nat. Commun.* **12**, 6047. (doi:10.1038/s41467-021-26309-5)

139. Millar TJ. 2003 Deuterium fractionation in interstellar clouds. *Space Sci. Rev.* **106**, 73–86. (doi:10.1023/A:1024677318645)

140. Herbst E. 2003 Isotopic fractionation by ion-molecule reactions. *Space Sci. Rev.* **106**, 293–304. (doi:10.1023/A:1024654108167)

141. Petralia LS, Tsikritea A, Loreau J, Softley TP, Heazlewood BR. 2020 Strong inverse kinetic isotope effect observed in ammonia charge exchange reactions. *Nat. Commun.* **11**, 173. (doi:10.1038/s41467-019-13976-8)

142. Tsikritea A, Park K, Bertier P, Loreau J, Softley TP, Heazlewood BR. 2021 Inverse kinetic isotope effects in the charge transfer reactions of ammonia with rare gas ions'. *Chem. Sci.* **12**, 10 005–10 013. (doi:10.1039/D1SC01652K)

143. Meyer KAE, Pollum LLL, Petralia LS, Tauschinsky A, Rennick CJ, Softley TP, Heazlewood BR. 2015 Ejection of Coulomb crystals from a linear Paul ion trap for ion–molecule reaction studies. *J. Phys. Chem. A* **119**, 12 449–12 456. (doi:10.1021/acs.jpca.5b07919)

144. Krohn OA, Catani KJ, Lewandowski HJ. 2022 Formation of astrochemically relevant molecular ions: reaction of translationally cold CCl^+ with benzene in a linear ion trap. *Phys. Rev. A* **105**, L020801. (doi:10.1103/PhysRevA.105.L020801)

145. Yang T, Li A, Chen GK, Yao Q, Suits AG, Guo H, Hudson ER, Campbell WC. 2021 Isomer-specific kinetics of the $C^+ + H_2O$ reaction at the temperature of interstellar clouds. *Sci. Adv.* **7**, eabe4080. (doi:10.1126/sciadv.abe4080)

146. Wild R, Nötzold M, Simpson M, Tran TD and Wester R. 2023 Tunnelling measured in a very slow ion–molecule reaction. *Nature* **615**, 425–429. (doi:10.1038/s41586-023-05727-z)

147. Hu MG *et al.* 2019 Direct observation of bimolecular reactions of ultracold KRb molecules. *Science* **366**, 1111–1115. (doi:10.1126/science.aay9531)

148. Hu M-G, Liu Y, Nichols MA, Zhu L, Quéméner G, Dulieu O, Ni K-K. 2021 Nuclear spin conservation enables state-to-state control of ultracold molecular reactions. *Nat. Chem.* **13**, 435–440. (doi:10.1038/s41557-020-00610-0)

149. Quack M. 1977 Detailed symmetry selection rules for reactive collisions. *Mol. Phys.* **34**, 477–504. (doi:10.1080/00268977700101861)

150. Man MP, Groenenboom GC, Karman T. 2022 Symmetry breaking in sticky collisions between ultracold molecules. (http://arxiv.org/abs/2203.13598v2)

151. Croft JFE, Bohn JL. 2021 Anomalous lifetimes of ultracold complexes decaying into a single channel: what's taking so long in there? (http://arxiv.org/abs/2111.09956v1)

152. Liu Y, Hu M-G, Nichols MA, Grimes DD, Karman T, Guo H, Ni K-K. 2020 Photo-excitation of long-lived transient intermediates in ultracold reactions. *Nat. Phys.* **16**, 1132–1136. (doi:10.1038/s41567-020-0968-8)

153. Gregory PD, Blackmore JA, Bromley SL, Cornish SL. 2020 Loss of ultracold $^{87}Rb^{133}Cs$ molecules via optical excitation of long-lived two-body collision complexes. *Phys. Rev. Lett.* **124**, 163402. (doi:10.1103/PhysRevLett.124.163402)

154. de Miranda MHG, Chotia A, Neyenhuis B, Wang D, Quéméner G, Ospelkaus S, Bohn JL, Ye J, Jin DS. 2011 Controlling the quantum stereodynamics of ultracold bimolecular reactions. *Nat. Phys.* **7**, 502–507. (doi:10.1038/nphys1939)

155. Tobias WJ, Matsuda K, Li JR, Miller C, Carroll AN, Bilitewski T, Rey AM, Ye J. 2022 Reactions between layer-resolved molecules mediated by dipolar spin exchange. *Science* **375**, 1299–1303. (doi:10.1126/science.abn8525)

156. Schuster T, Flicker F, Li M, Kotochigova S, Moore JE, Ye J, Yao NY. 2021 Floquet engineering ultracold polar molecules to simulate topological insulators. *Phys. Rev. A* **103**, 063322. (doi:10.1103/PhysRevA.103.063322)

157. Reynolds LA, Schwartz E, Ebling U, Weyland M, Brand J, Andersen MF. 2020 Direct measurements of collisional dynamics in cold atom triads. *Phys. Rev. Lett.* **124**, 073401. (doi:10.1103/PhysRevLett.124.073401)

158. Anderegg L, Burchesky S, Bao Y, Yu SS, Karman T, Chae E, Ni K-K, Ketterle W, Doyle JM. 2021 Observation of microwave shielding of ultracold molecules. *Science* **373**, 779–782. (doi:10.1126/science.abg9502)

159. De Mille D. 2002 Quantum computation with trapped polar molecules. *Phys. Rev. Lett.* **88**, 067901. (doi:10.1103/PhysRevLett.88.067901)

160. Altman E *et al.* 2021 Quantum simulators: architectures and opportunities. *PRX Quantum* **2**, 017003. (doi:10.1103/PRXQuantum.2.017003)

161. Gregory PD, Blackmore JA, Bromley SL, Hutson JM, Cornish SL. 2021 Robust storage cubits in ultracold polar molecules. *Nat. Phys.* **17**, 1149–1152. (doi:10.1038/s41567-021-01328-7)

162. Burchesky S, Anderegg L, Bao Y, Yu SS, Chae E, Ketterle W, Ni K-K, Doyle JM. 2021 Rotational coherence times of polar molecules in optical tweezers. *Phys. Rev. Lett.* **127**, 123202. (doi:10.1103/PhysRevLett.127.123202)

163. Sawant R, Blackmore JA, Gregory PD, Mur-Petit J, Jaksch D, Aldegunde J, Hutson JM, Tarbutt MR, Cornish SL. 2020 Ultracold polar molecules as qudits. *New J. Phys.* **22**, 013027. (doi:10.1088/1367–2630/ab60f4)

164. Zhu G-Z, Lao G, Ho C, Campbell WC, Hudson ER. 2022 High-resolution laser-induced fluorescence spectroscopy of $^{28}Si^{16}O^+$ and $^{29}Si^{16}O^+$ in a cryogenic buffer-gas cell. *J. Mol. Spectrosc.* **384**, 111582. (doi:10.1016/j.jms.2022.111582)

165. Yao NY, Zaletel MP, Stamper-Kurn DM, Vishwanath A. 2018 A quantum dipolar spin liquid. *Nat. Phys.* **14**, 405–410. (doi:10.1038/s41567-017-0030-7)

166. Syzranov SV, Wall ML, Zhu B, Gurarie V, Rey AM. 2016 Emergent Weyl excitations in systems of polar particles. *Nat. Commun.* **7**, 13543. (doi:10.1038/ncomms13543)

167. Yao NY, Gorshkov AV, Laumann CR, Läuchli AM, Ye J, Lukin MD. 2013 Realizing fractional Chern insulators in dipolar spin systems. *Phys. Rev. Lett.* **110**, 185302. (doi:10.1103/PhysRevLett.110.185302)

168. Rasdijk O *et al.* 2021 CeNTREX: a new search for time-reversal symmetry violation in the ^{205}Tl nucleus. *Quantum Sci. Technol.* **6**, 044007. (doi:10.1088/2058-9565/abdca3)

169. Andreev V *et al.* 2018 Improved limit on the electric dipole moment of the electron. *Nature* **562**, 355. (doi:10.1038/s41586-018-0599-8)

170. Zhou Y *et al.* 2020 Second-scale coherence measured at the quantum projection noise limit with hundreds of molecular ions. *Phys. Rev. Lett.* **124**, 053201. (doi:10.1103/PhysRevLett.124.053201)

171. Roussy TS *et al.* 2022 A new bound on the electron's electric dipole moment. (http://arxiv.org/abs/2212.11841v3)

172. Cheng C, van der Poel APP, Jansen P, Quintero-Pérez M, Wall TE, Ubachs W, Bethlem HL. 2016 Molecular fountain. *Phys. Rev. Lett.* **117**, 253201. (doi:10.1103/PhysRevLett.117.253201)

173. Patterson D, Schnell M, Doyle JM. 2013 Enantiomer-specific detection of chiral molecules via microwave spectroscopy. *Nature* **497**, 475–477. (doi:10.1038/nature12150)

174. Erez I, Wallach ER, Shagam Y. 2022 Simultaneous enantiomer-resolved Ramsey spectroscopy for chiral molecules. (http://arxiv.org/abs/2206.03699v1)

175. Lara M, Jambrina PG, Aoiz FJ, Launay J-M. 2015 Cold and ultracold dynamics of the barrierless $D^+ + H_2$ reaction: quantum reactive calculations for $\sim R^{-4}$ long range interaction potentials. *J. Chem. Phys.* **143**, 204305. (doi:10.1063/1.4936144)

176. Dieterle T, Berngruber M, Hölzl C, Löw R, Jachymski K, Pfau T, Meinert F. 2021 Tracking diffusive motion of single Rb^+ ion formed in a Rb BEC. *Phys. Rev. Lett.* **126**, 033401. (doi:10.1103/PhysRevLett.126.033401)